

## Airway Anomalies, Lung and Mediastinal Masses, and Hydrothorax

Richard A. Barth

### AIRWAY ANOMALIES

#### Congenital High Airway Obstruction Syndrome

Congenital high airway obstruction syndrome (CHAOS) is a rare fetal anomaly resulting from airway obstruction secondary to laryngeal atresia, or less commonly a laryngeal cyst, laryngeal web, laryngeal stenosis, or tracheal atresia.<sup>1,2</sup> CHAOS is typically bilateral; however, sporadically can be unilateral secondary to central bronchial atresia.

**Incidence:** The incidence of CHAOS is unknown as only a few cases have been reported in the literature.<sup>3,4</sup>

**Pathogenesis/Associated Anomalies:** The pathogenesis relates to a complete airway obstruction resulting in trapping and accumulation of fluid within the fetal airways and lungs. Pathologic findings include severe distention of the fetal trachea, bronchi, and hyperplastic lungs. The markedly enlarged

fetal lungs compress the heart and inferior vena cava decreasing venous return to the heart, which often results in fetal ascites, in-utero heart failure, placentomegaly, and hydrops fetalis.<sup>1</sup> Isolated CHAOS is a sporadic fetal malformation with a low risk for associated anomalies or chromosomal abnormalities. Less-commonly CHAOS can be associated with Fraser syndrome, which is an autosomal recessive disorder characterized by laryngeal atresia secondary to underlying fusion of the false vocal cords. Other associations with Fraser syndrome include renal agenesis, microphthalmia, cryptophthalmos, polydactyly, syndactyly, cleft lip/palate, ear anomalies, ambiguous genitalia, congenital heart disease, and severe oligohydramnios secondary to bilateral renal agenesis.<sup>5,6</sup>

**Diagnosis:** On ultrasound (US), the characteristic findings of CHAOS include hyperechogenic and hyperexpanded lungs resulting in flattening or inversion of the diaphragms (Fig. 17.3-1A,B).<sup>3,6</sup> A dilated fluid-filled trachea and bronchi are often identified below the level of the airway obstruction, which most commonly occurs at the level of the larynx. Color Doppler will allow separation of the dilated airway from adjacent vasculature. Fetal ascites is a common feature of CHAOS resulting from obstructed venous return to the heart.

On magnetic resonance imaging (MRI), T2-weighted sequences show similar findings including hyperinflated high-signal lungs inverting diaphragms and severely dilated bronchi distal to the more proximal airway obstruction (see Fig. 17.3-1C,D).

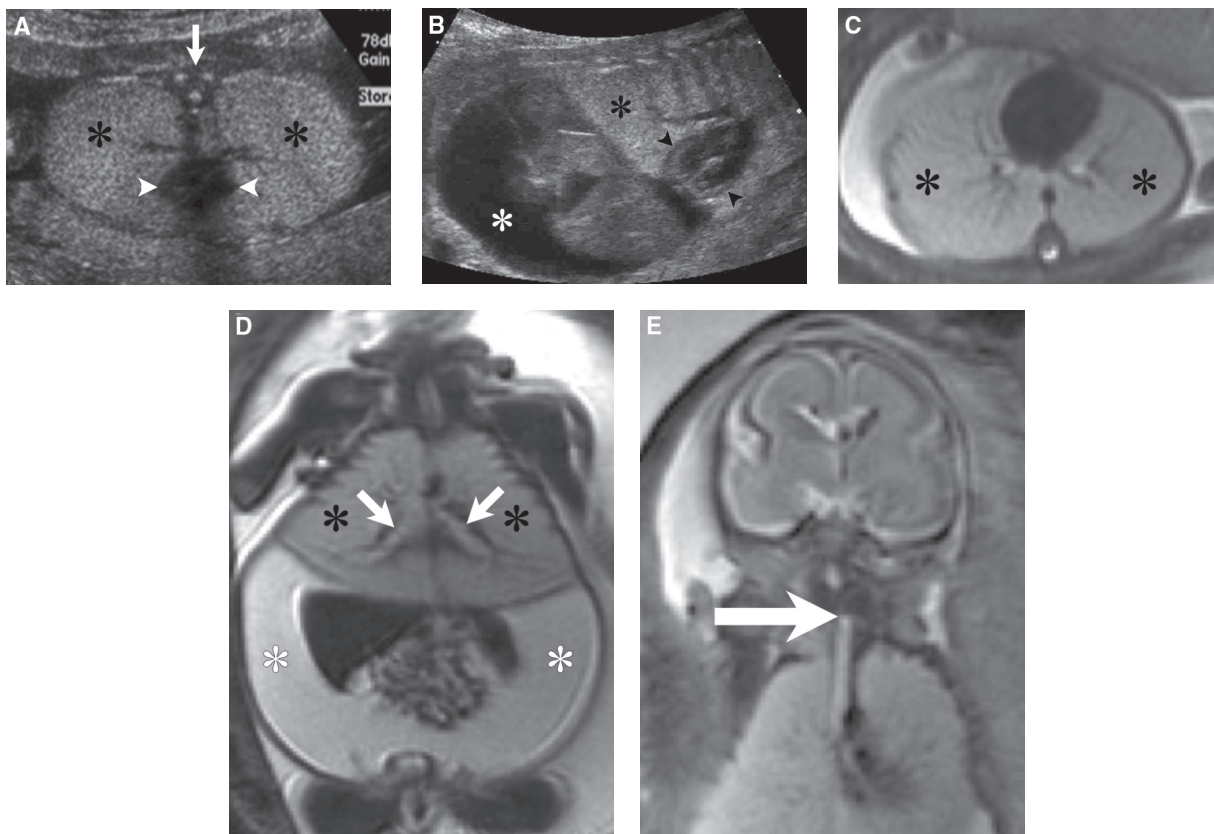


**FIGURE 17.3-1:** CHAOS in 25-week gestational age fetus. Axial (A) and sagittal (B) plane US images through the fetal chest demonstrate hyperinflated lungs (black asterisks), a compressed heart (arrowheads), and fetal ascites (B, white asterisk). Arrow indicates the spine. Axial (C) and coronal (D) plane T2-weighted MR images demonstrate enlarged hyperintense lungs (black asterisks), distended airways (arrows), inverted diaphragms, and fetal ascites (white asterisks). E: Coronal MRI demonstrates precise level of obstruction at the level of the fetal larynx (arrow).

Fetal ascites is also frequently seen. MRI may compliment US by demonstrating the precise level of airway obstruction in preparation for the mandatory tracheostomy required as a lifesaving intervention during the delivery process (see Fig. 17.3-1E).

**Differential Diagnosis:** Congenital pulmonary airway malformation (CPAM) is the primary differential diagnosis. In distinction to CHAOS, the majority of CPAMs are unilateral lesions; however, the rare case of bilateral-type 3 microcystic CPAM or the even rarer variant of type 0 CPAM composed of acinar dysplasia affecting all lobes may appear similar to CHAOS.<sup>7,8</sup>

**Prognosis:** CHAOS is usually a lethal anomaly with mortality in approximately 80% to 100% of cases.<sup>1</sup> This is especially true when CHAOS is associated with Fraser syndrome. In the absence of additional congenital malformations, prognosis depends on lung size and presence of hydrops. In the absence of hydrops, some cases may be salvageable with proper perinatal management. Rarely, a spontaneous in utero fistula between the obstructed airway and esophagus may develop, improving survival postnatal.

**Management:** In most cases, the natural history of CHAOS includes a progressive enlargement of both lungs with secondary hydrops and a high association with perinatal demise. Termination of pregnancy is a reasonable option to be discussed with the parents. The perinatal outcome of CHAOS is 100% mortality without intervention to secure an airway. Fetuses with CHAOS may benefit from in-utero fetal therapy via a fetoscopic tracheostomy to ameliorate the intrapulmonary hyperexpansion, and to provide mediastinal decompression thereby improving venous return to the heart.<sup>9</sup> The only viable perinatal management option to improve survival is delivery via the ex utero intrapartum treatment (EXIT) procedure.<sup>10,11</sup> Even with tracheostomy and delivery via the EXIT procedure only a few survivors have been reported.<sup>1,10,11</sup>

**Recurrence:** Isolated CHAOS is a sporadic event with no known recurrence risk.

## Emphysema/Overinflation

### Congenital Lobar Overinflation

Congenital lobar overinflation (CLO; aka congenital lobar emphysema) is an overinflation of a lung lobe, characterized on microscopic analysis by air space enlargement without maldevelopment.<sup>12</sup> Congenital lung overinflation is likely a better descriptor than congenital lobar overinflation as the abnormality often involves only a lung segment or subsegment. The designation of overinflation is preferred to that of emphysema since the lung is hyperinflated, with intact alveolar walls.

**Incidence:** Overinflation accounts for approximately 20% of all prenatally diagnosed fetal lung malformations (Table 17.3-1).<sup>13</sup>

**Pathogenesis:** Pathologically, CLO is composed of two subgroups. The first group is associated with an overinflated lung lobe caused by an intrinsic cartilage abnormality of the airway, absent bronchial cartilage, or extrinsic compression of the airway by an enlarged pulmonary artery or bronchogenic cyst.<sup>14</sup> The collapsed airway acts as a one-way valve resulting in air

Table 17.3-1

### Distribution of Pathologically Proven Fetal Lung Lesions (108 Cases)

CPAM	47%
Hybrid (CPAM and sequestration)	25%
Overinflation/bronchial atresia	20%
Sequestration	8%

Adapted from Epelman M, Kreiger PA, Servaes S, et al. Current imaging of prenatally diagnosed congenital lung lesions. *Semin Ultrasound CT MR*. 2010;31:141–157.

trapping, and historically, the majority of cases presented with respiratory distress in the newborn or infant. This form of CLO, previously known as CLE, occurs most frequently in the left upper lobe followed by the right middle and right upper lobes with the lower lobes involved in less than 1% of cases.<sup>15</sup> A second subgroup of overinflation patients has emerged largely via prenatal diagnosis. This group is characterized by lobar, segmental, or subsegmental overinflation and a high association with bronchial atresia. This subgroup has a predisposition to the lower lobes and lower symptomatology.<sup>16</sup>

**Diagnosis:** On prenatal US, CLO appears as a primarily homogeneous hyperechogenic mass compared with normal lung tissue (Fig. 17.3-2A). A central dilated bronchus distal to an atretic bronchus helps to confirm the diagnosis of associated bronchial atresia/anomaly.<sup>15,16</sup> In addition, mass effect with mediastinal shift may be identified. On color Doppler, CLO demonstrates blood supply from the pulmonary artery and drainage via the pulmonary vein.<sup>17</sup>

On MRI T2-weighted images, CLO typically appears as a homogeneous high-signal lung mass compared with normal lung tissue (see Fig. 17.3-2B,C). On MRI, it is often possible to identify the central dilated mucoid impacted bronchus distal to an atretic or abnormal bronchus (see Fig. 17.3-2D).

**Differential Diagnosis:** The microcystic form of CPAM is the primary differential diagnosis for CLO. Microcystic CPAM appears similar on US and MRI, and is often an incorrect default prenatal diagnosis when an echogenic mass is detected on US. Pacharn et al.<sup>18</sup> reported high accuracy of prenatal MRI for the diagnosis of the specific type of bronchopulmonary malformation (BPM) with postnatal confirmation of the correct diagnosis on pathology or postnatal imaging in 96% of the cases utilizing a designated algorithm (Fig. 17.2-3). On MRI, CPAMs may have a more heterogeneous appearance associated with small cystic areas. Identification of a central dilated bronchus suggests bronchial atresia and favors the diagnosis of CLO. Bronchopulmonary sequestrations (BPSs) may also appear similar to CLO on US and MRI; however, identification of a systemic arterial feeder in a sequestration should allow for accurate diagnosis.

**Prognosis:** Prenatal complications and postnatal sequelae of prenatally diagnosed CLO are rare. The majority of prenatally diagnosed CLO cases are asymptomatic at birth.<sup>16</sup>

**Management:** Prenatal management of CLO consists of serial USs to assess for the infrequent case associated with a large degree of mass effect, which is more likely to be associated with respiratory distress at birth. Fetal intervention is rarely indicated

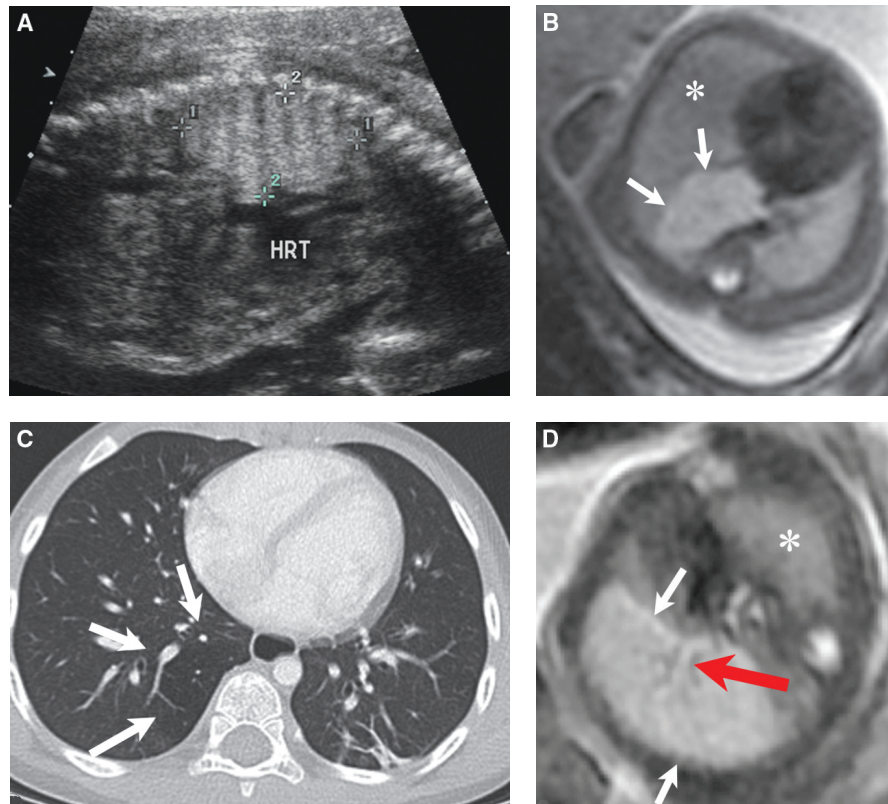


**FIGURE 17.3-2:** CLO in 22-week gestational age fetus. **A:** Sagittal plane US through the fetal chest demonstrates a homogeneous hyperechogenic mass in the right lower lobe (*calipers*). HRT, heart. **B:** Axial plane T2-weighted MRI demonstrates a homogeneous high-signal intensity mass (*arrows*) in the right lower lung (*asterisk*). **C:** CT in the same patient as a newborn demonstrates a hyperlucent segment in the right lower lobe (*arrows*) with otherwise normal architecture. **D:** Axial T2-weighted MRI in different fetus with confirmed right lower lobe congenital lung overinflation (*white arrows*) and bronchial atresia. Dilated mucoid impacted bronchus (*red arrow*). Asterisk indicates normal lung.

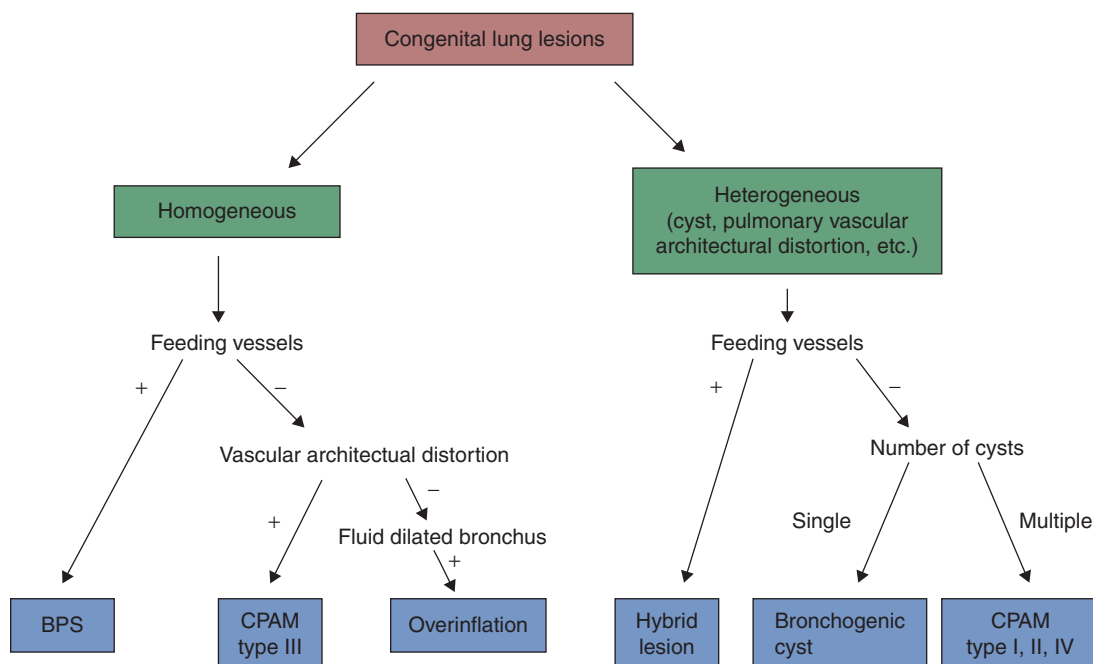


**FIGURE 17.3-3:** Algorithm for diagnosing lung lesions on fetal MRI. (Adapted from Pacharn P, Kline-Fath B, Calvo-Garcia M, et al. Congenital lung lesions: comparison between prenatal magnetic resonance imaging (MRI) and postnatal findings. In: Radiological Society of North America 95th Scientific Assembly & Annual Meeting; November 29–December 4, 2009; Chicago, IL.)

for CLO. Accurate diagnosis of CLO is important since the incidence of fetal and postnatal complications are uncommon compared with CPAM, and the postnatal management of asymptomatic CLO may be conservative without surgical intervention.

**Recurrence:** There is no known recurrence risk for isolated congenital lobar overinflation.

**Esophageal Atresia/Tracheoesophageal Fistula**

Esophageal atresia is characterized by interruption of the esophagus, resulting in a blind-ending pouch. Often, there is an associated fistula between the trachea and the esophagus.

**Incidence:** The incidence of esophageal atresia is approximately 1:4,000 live births.<sup>19,20</sup> More than 90% have an associated tracheoesophageal fistula.<sup>21,22</sup>

**Pathogenesis/Associated Anomalies:** Esophageal atresia results when the tracheoesophageal septum of the foregut fails to complete division of the foregut into the ventral respiratory and dorsal digestive portions. Esophageal atresia can be subclassified into five major types (Fig. 17.3-4). Type A is the most common anatomic configuration, representing proximal esophageal atresia with a tracheoesophageal fistula to the distal esophageal segment. The other types of esophageal atresia

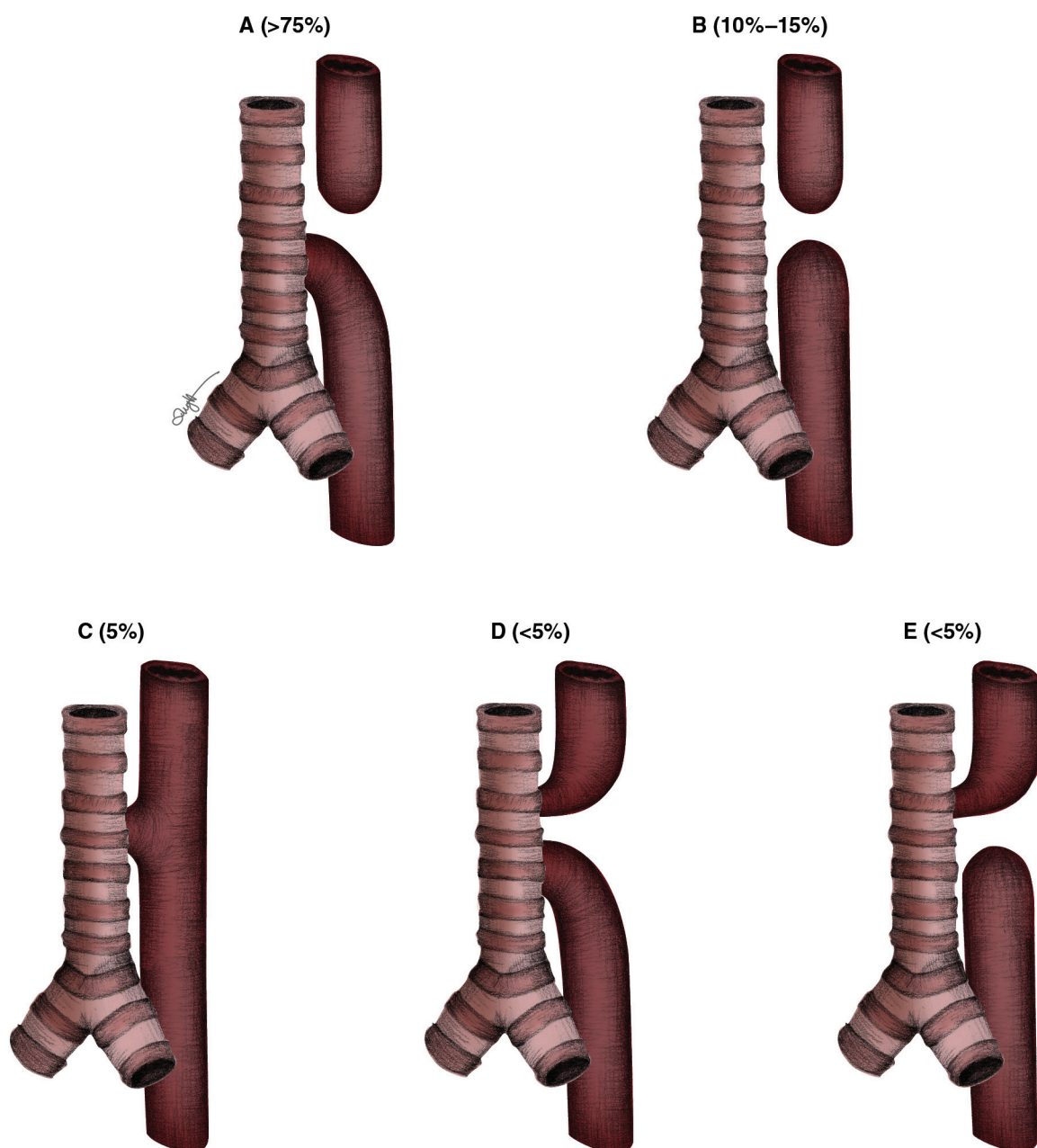


**FIGURE 17.3-4:** Five subtypes of tracheoesophageal fistula and esophageal atresia. **A:** Esophageal atresia with distal tracheoesophageal fistula. **B:** Esophageal atresia with no tracheoesophageal fistula. **C:** H-type tracheoesophageal fistula with no esophageal atresia. **D:** Esophageal atresia with both proximal and distal tracheoesophageal fistulas. **E:** Esophageal atresia with proximal tracheoesophageal fistula.

in decreasing order of frequency are: Type B: Esophageal atresia without tracheoesophageal fistula; Type C: Tracheoesophageal fistula with no esophageal atresia; Type D: Esophageal atresia with tracheoesophageal fistula to both the proximal and the distal esophageal segments; and Type E: Esophageal atresia with tracheoesophageal fistula to the proximal esophageal segment.

Other associated malformations are seen in up to 70% of fetuses with esophageal atresia with the incidence for the most frequent abnormalities as follows: cardiovascular (35%) (most commonly PDA and VSD), gastrointestinal (24%) (most commonly anal atresia and duodenal atresia), genitourinary (20%) (most commonly unilateral renal agenesis or renal dysplasia), skeletal (13%) (most commonly vertebral, rib, or radial ray), and neurologic (10%) (most commonly hydrocephalus).<sup>19,21-24</sup> Esophageal atresia may also occur in association with other gastrointestinal tract atresias.<sup>25,26</sup> The association of esophageal atresia and duodenal atresia in the absence of a tracheoesophageal fistula results in a closed loop bowel obstruction involving the distal esophagus, stomach, and duodenum.<sup>27</sup> Approximately 10% of cases of esophageal atresia are part of the VACTERL association (Vertebral anomalies, Anal atresia, Cardiac anomalies, Tracheoesophageal fistula, Renal anomalies, and Limb anomalies).<sup>28,29</sup> Careful search for these associated anomalies should be performed on prenatal US and MRI when esophageal atresia is suspected.

Aneuploidy, most commonly trisomy 18 and 21, is relatively common in esophageal atresia ranging from 5% to 10% in different series.<sup>28,30</sup> The risk of trisomy 21 is 30 times higher than expected in the general population.<sup>21,31,32</sup>

**Diagnosis:** Prenatal US detection of esophageal atresia is challenging; however, the constellation of a small or absent stomach, polyhydramnios, and a pouch sign is highly suggestive of esophageal atresia (Fig. 17.3-5A).<sup>33,34</sup> The pouch sign represents the proximal fluid-containing esophageal blind pouch located in the neck or the superior mediastinum. The detection of the proximal esophageal pouch is not straightforward because it fills and empties periodically, likely related to fetal swallowing. Furthermore, depending on the nature of the anomaly, the pouch may

be located in the cervical region or superior mediastinum. The sensitivity and accuracy for identifying the proximal esophageal pouch has not been carefully examined. Diagnosis of esophageal atresia with an absent stomach and polyhydramnios is rare prior to 22 weeks' gestation. In fact, a normal appearing stomach and a normal amount of amniotic fluid may be seen earlier in gestation. Overall sensitivity for detecting esophageal atresia associated with tracheoesophageal fistula is low, cited at 30% prenatal detection rate.<sup>35,36</sup> Limited detection may be explained by the fact that in the presence of esophageal atresia with tracheoesophageal fistula, the stomach may fill with fluid via the fistula. It is possible that in many cases of esophageal atresia, the tracheoesophageal fistula maintains flow into the stomach early in pregnancy, but that the fistula progressively narrows as pregnancy continues, resulting in a small or non visualized stomach.

Stringer et al.<sup>35</sup> reported a predictive value for esophageal atresia ranging from 39% with identification of a small stomach and polyhydramnios to 56% for polyhydramnios in the absence of an identifiable fetal stomach. When esophageal atresia without a tracheoesophageal fistula is associated with duodenal atresia, US will typically reveal significant polyhydramnios in association with a severely distended stomach because of the closed loop obstruction.<sup>27,37</sup>

MRI may demonstrate a proximal fluid-filled blind-ending esophageal pouch on T2-weighted sequences, which can be difficult to detect on US (see Fig. 17.3-5B,C). MRI may also rarely identify the tracheoesophageal fistula. Although MRI may increase the accuracy of diagnosis, the current MRI data are mainly from case reports with no large series yet available.<sup>32,36,38</sup> MRI may also be useful to identify associated anomalies not definitively diagnosed on US, including anal atresia and vertebral anomalies.

**Differential Diagnosis:** Non visualization of the fetal stomach has been reported in approximately 0.07% to 0.4% of pregnancies with abnormal outcome in 48% to 100% of the cases.<sup>39,40</sup> In addition to esophageal atresia, lack of visualization of the fluid-filled stomach may be seen in conditions associated with abnormal swallowing and passage of amniotic fluid into the esophagus and stomach, including severe fetal central nervous

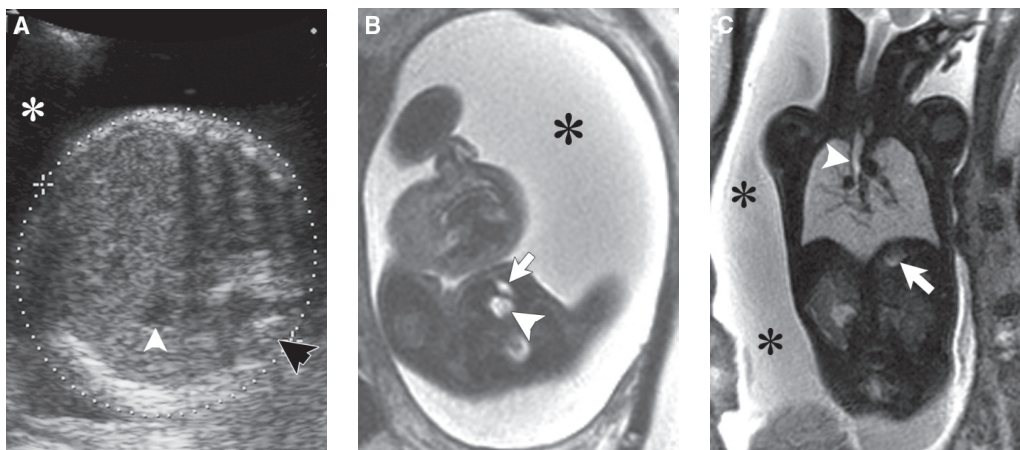


**FIGURE 17.3-5:** Esophageal atresia with tracheoesophageal fistula in 30-week gestational age fetus. **A:** Axial sonogram through the upper abdomen demonstrates a very small fetal stomach (*white arrowhead*) and polyhydramnios (*asterisks*). The spine is indicated by *black arrowhead*. T2-weighted MRI axial scan through the neck (**B**) and coronal view of the chest (**C**) demonstrate the proximal esophageal pouch (*arrowheads*), posterior to the trachea (*arrow* in C), and polyhydramnios (*asterisks*). The *arrow* in C indicates the small stomach.

system disorders, neck masses (particularly anterior neck teratomas or fetal goiter), anatomic disorders of swallowing (such as severe cleft palate), diaphragmatic hernia with an intrathoracic stomach, and any cause of oligohydramnios, which limits the available fluid for swallowing.

A small stomach may also be seen with congenital microgastria, which is an extremely rare anomaly believed to result from impairment of normal foregut development. On sonography, these cases demonstrate a very small stomach on serial scans. Of note, in congenital microgastria, the amniotic fluid may be normal, whereas in esophageal atresia, polyhydramnios is usually present late in gestation.<sup>41-43</sup>

**Prognosis:** The outcome of fetuses and infants with esophageal atresia has been reported as unfavorable with perinatal mortality of 21%, primarily as a result of associated congenital malformations and prematurity.<sup>19,44-46</sup>

Morbidity in survivors depends mostly on the timing of diagnosis and the presence of associated anomalies. Postoperative mortality in infants surviving to undergo primary surgery has been reported at 9%.<sup>19</sup> The prognosis for esophageal atresia without associated anomalies or genetic disorder is good.

**Management:** All patients suspected to have esophageal atresia should undergo genetic counseling and referred for karyotype evaluation given the increased risk for trisomies 18 and 21. In addition, all patients should undergo a fetal cardiac echo to assess for associated cardiac anomalies. Esophageal atresia is usually well managed after birth with surgical correction, and therefore fetal intervention is not indicated.<sup>44</sup>

**Recurrence:** Esophageal atresia can occur as an isolated finding, as part of a genetic syndrome, or as part of a non isolated (but not syndromic) set of findings. Most individuals with esophageal atresia are the only affected member of the family, and when esophageal atresia is the only abnormality without a clear etiology, the recurrence risk for siblings is approximately 1%.<sup>47</sup> When esophageal atresia is associated with an inherited chromosomal abnormality or specific syndrome, genetic counseling for recurrence risk is indicated.<sup>47</sup>

## LUNG LESIONS

### Congenital Pulmonary Airway Malformation (aka Congenital Cystic Adenomatoid Malformation)

Congenital pulmonary airway malformations are part of the bronchopulmonary malformation (BPM) spectrum, which include BPS, hybrid lesions (CPAM and sequestration), and CLO/bronchial atresia.

**Incidence:** CPAMs are the most common lung anomaly diagnosed in the fetus, accounting for approximately half of all lesions (see Table 17.3-1).<sup>13</sup> The estimated incidence for prenatal diagnosis is 1:4,000 to 1:6,000 pregnancies.<sup>48,49</sup>

**Pathogenesis:** The definite etiology is unknown but several mechanisms have been referenced. A gene interaction (Hox B-5; FGF-7; PDGFB Gene) has been a suggested cause of CPAMs.<sup>50,51</sup> Homeobox genes control axial identity and organ-specific patterning during embryogenesis.<sup>52</sup> Abnormal Hox B-5 expression during human lung branching morphogenesis

has been implicated in the development of CPAMs.<sup>50,51</sup> Airway obstruction in the developing fetus has also been cited as the etiology of most BPMs, with the type of malformation depending on the severity and timing of airway obstruction during lung development.<sup>12,53,54</sup> Supporting this conclusion is the associated pathologic diagnosis of bronchial atresia in 70% of CPAMs.<sup>53</sup>

CPAMs represent a benign hamartomatous or dysplastic tumor, which are composed of a mass of abnormal solid or cystic pulmonary tissue in which there is proliferation of bronchial structures at the expense of alveolar development. These lesions are thought to result from abnormal endodermal and mesodermal differentiation between the 5th to 7th week of gestation.

These lesions typically involve one pulmonary lobe and usually communicate with the tracheobronchial tree, although the communication is abnormal. CPAMs receive blood supply from the pulmonary artery and drain via the pulmonary veins with the exception of hybrid lesions (CPAM and sequestration), which also have a systemic arterial blood supply. CPAMs may be predominately cystic, solid, or mixed pathologically.

Stocker et al.<sup>49</sup> has pathologically classified CPAMs into three types according to cyst size and histologic resemblance to the segments of the developing bronchial tree and airspaces (Fig. 17.3-6). Type I macrocystic CPAM lesions are characterized by single or multiple cysts greater than 2 cm in diameter lined by ciliated pseudo stratified columnar epithelium.<sup>55</sup> These account for approximately half of all CPAM lesions in postnatal series.<sup>55</sup> Type II lesions are characterized by macroscopic cysts ranging from 0.5 to 2.0 cm in diameter and lined with mixed ciliary, columnar, and cuboidal epithelium.<sup>55</sup> Type III lesions are predominately solid with microcystic components and are histologically composed of alveolus-like structures lined by ciliated cuboidal epithelium.<sup>55</sup> Type III CPAM comprises approximately 10% of all CPAMs. Type I lesions represent an anomaly of the more proximal bronchial tree affecting primarily the bronchioles, whereas type III lesions affect the more distal portion of the bronchial tree at the level of the alveoli.<sup>56</sup> Recently, two additional subtypes of CPAM have been added to the classification (types 0 and 4).<sup>55</sup> Type 0 is characterized by acinar dysplasia or agenesis and is very rare, involving all of the lung lobes, and is incompatible with postnatal survival.<sup>55</sup> Type 4 lesions, which cannot be differentiated from Type I and 2 lesions by imaging,

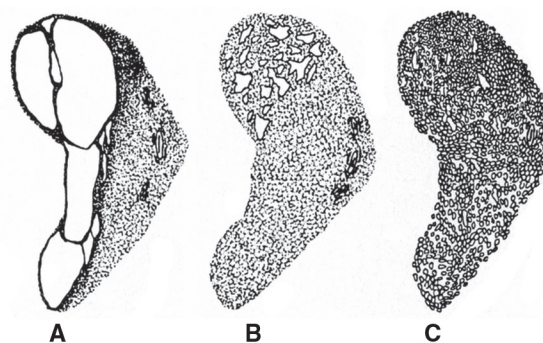


**FIGURE 17.3-6:** The three original types of congenital pulmonary airway malformation of the fetus as described by Stocker et al.<sup>49</sup> **A:** Type I lesions have large cysts of variable sizes. **B:** Type II lesions have smaller cysts. **C:** Type III lesions are microcystic and appear solid on US owing to reflections from numerous microscopically dilated bronchioles. (Redrawn from Stocker JT, Madewell JE, Drake RM. Congenital cystic adenomatoid malformation of the lung: classification and morphologic spectrum. *Hum Pathol.* 1977;8:155-171. Copyright 1977 Elsevier.)

are characterized by large peripheral cysts of the distal acinus lined predominately by alveolar-type cells. With this new classification, Stocker<sup>55</sup> proposed that the prior designation of congenital cystic adenomatoid malformation (CCAM) be changed to CPAM as the lesions are cystic in only three of the five pathological classifications and adenomatoid in one type.

**Diagnosis:** On prenatal US, most CPAMs are detected as an incidental finding. CPAMs may appear as a predominately macrocystic mass, microcystic hyperechogenic solid mass, or a complex mass with both cystic and echogenic components (Fig. 17.3-7). Solid masses are typically hyperechogenic compared with normal fetal lung in the second trimester, and often become isoechoic with the normal fetal lung and invisible on sonography in the third trimester (Fig. 17.3-8). The decreasing conspicuity relates to both the increasing echogenicity of the normal fetal lungs as pregnancy progresses and the propensity of solid masses to decrease in size as pregnancy progresses. When solid masses are isoechoic to normal lung, the sonographic diagnosis is more challenging and relies on mass effect, including mediastinal shift, altered cardiac position or axis, or an inverted diaphragm to confirm the diagnosis (Fig. 17.3-9A). Color Doppler US is useful in demonstrating pulmonary artery blood supply to the mass and drainage via the pulmonary vein (see Fig. 17.3-9B). Identification of an associated systematic arterial blood supply confirms the diagnosis of a hybrid

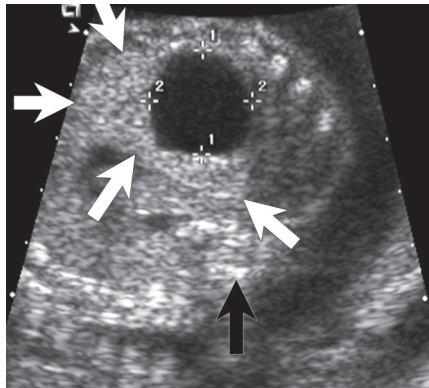


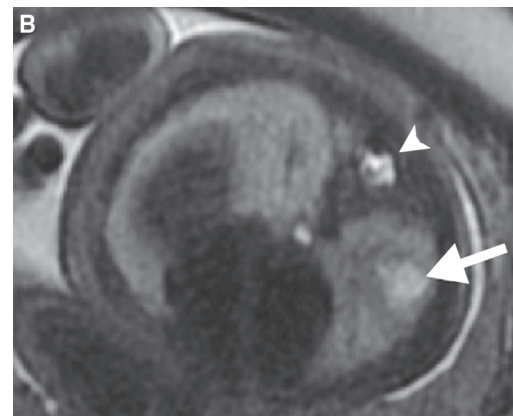
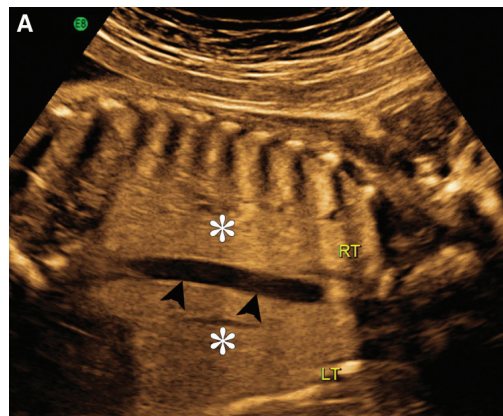
**FIGURE 17.3-7:** Complex cystic lung malformation detected as incidental finding on US at 22 weeks' gestational age. Axial sonogram through the fetal chest shows a complex mass composed of macrocystic (*calipers*) and solid (*white arrows*) components. Fetal spine is indicated by *black arrow*.

BPM composed of both CPAM and sequestration components (Fig. 17.3-10). Adzick<sup>57</sup> suggested a sonographic characterization based on a predominately macrocystic or microcystic appearance of CPAMs as a more clinically useful classification. The macrocystic lesions are composed of single or multiple cysts larger than 5 mm in diameter on US, and microcystic lesions appear as a solid hyperechogenic mass because of the numerous acoustic interfaces created by small cysts measuring less than 5 mm in diameter (Fig. 17.3-11).<sup>57</sup> The presence or absence of macroscopic cysts may be important as these can predispose to rapid growth and complications, and are also important in determining therapy for cases complicated by fetal hydrops. CPAMs are usually unilateral and unilobar with a slight predisposition to the lower lobes. Approximately 40% of CPAMs increase in size during pregnancy, with the most rapid growth occurring between 20 and 26 weeks' gestational age, after which growth peaks and plateaus.<sup>58,59</sup>

MRI may also be useful in the diagnosis and characterization of CPAMs. MRI is reported to provide alternative or additional diagnoses compared with US in 38% to 50% of fetuses with chest anomalies.<sup>38,60</sup> In the second trimester, CPAMs usually appear as a hyperintense mass compared with normal lung tissue on T2-weighted MRI sequences (Fig. 17.3-12A). CPAMs may appear high signal, isosignal, or lower signal compared with lung tissue in the third trimester of pregnancy. The identification of a high-signal mass alone on MRI is not specific for the type of bronchopulmonary malformation; however, identification of a macrocystic component and/or distortion of the vascular architecture is highly suggestive for CPAM (see Fig. 17.3-12B).<sup>38,61</sup> MRI may be useful during the third trimester of pregnancy in evaluating for pulmonary hypoplasia via lung volume measurements and confirming the presence and size of a CPAM when solid masses may not be visualized on US. In our experience, the latter is helpful in planning delivery location (see Fig. 17.3-8B). When the mass is ascertained to be small on MRI, patients can safely deliver in their local community and undergo elective evaluation of the mass after birth.

**Differential Diagnosis:** Differential diagnosis for a solid microcystic CPAM includes hybrid BPMs (CPAM and BPS), congenital lobar or segmental overinflation, and congenital diaphragmatic hernia. Solid hybrid lesions may be differentiated by identification of both pulmonary artery and systemic arterial blood supply to the mass on US or MRI. Lobar or segmental overinflation may appear similar to a CPAM on prenatal imaging.

**FIGURE 17.3-8:** Disappearing fetal lung mass in the third trimester. **A:** Coronal plane sonogram through the fetal chest shows no evidence of a fetal lung mass. Normal lungs are indicated by *asterisks* and the aorta by *arrowheads*. **B:** Axial plane fetal MRI confirms a small high-signal bronchopulmonary malformation (*arrow*). The *arrow-head* indicates the spine.



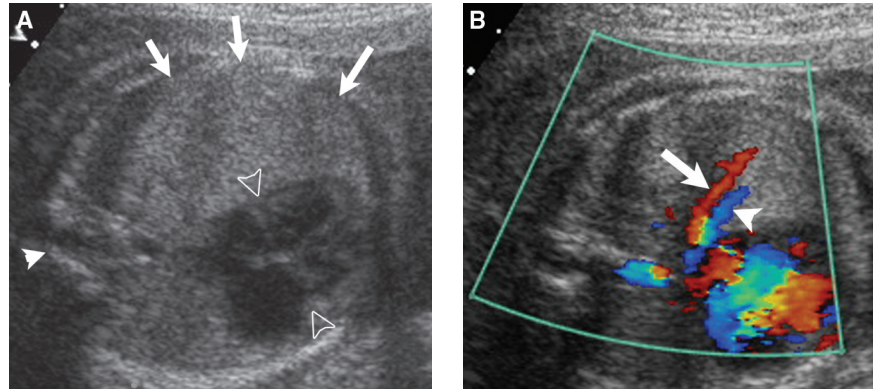


**FIGURE 17.3-9:** Isoechoic lung mass. **A:** Axial sonogram through the fetal chest demonstrates dextroposition of the heart (*open arrowheads*) secondary to an isoechoic lung mass (*arrows*). The spine is indicated by *closed arrowhead*. **B:** Axial plane Doppler sonogram demonstrates pulmonary artery blood supply to the mass (*arrow*) and drainage via the pulmonary vein (*arrowhead*). Postnatal surgical resection confirmed congenital pulmonary airway malformation.

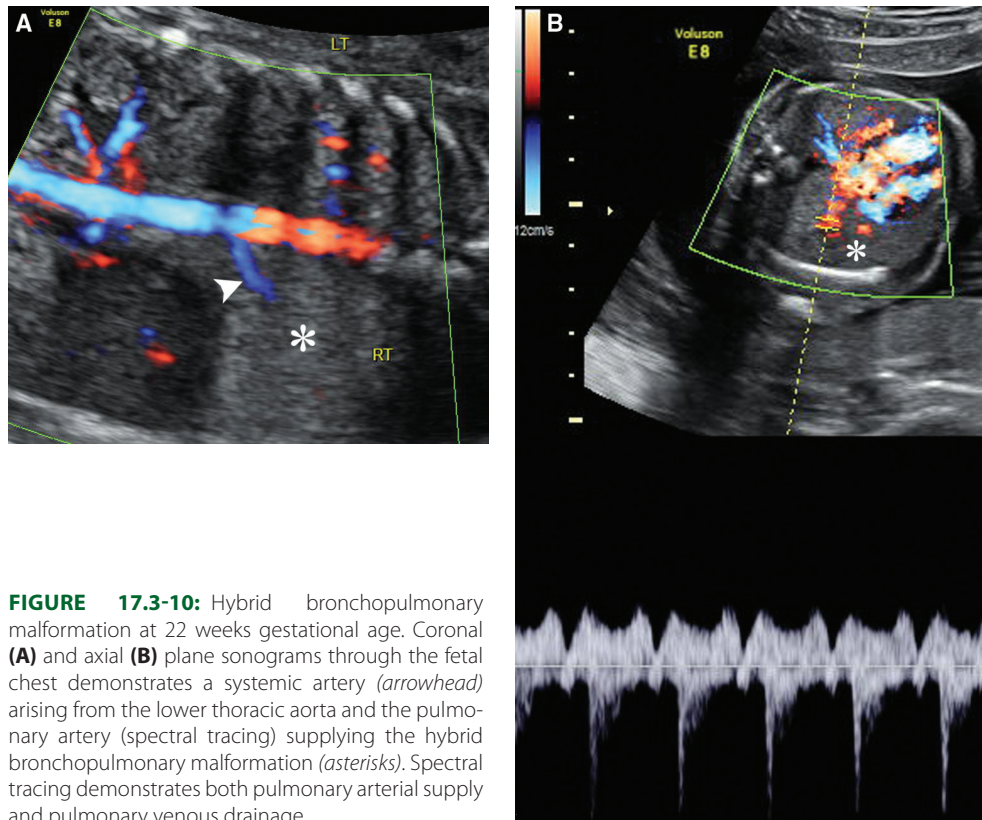


**FIGURE 17.3-10:** Hybrid bronchopulmonary malformation at 22 weeks gestational age. Coronal (**A**) and axial (**B**) plane sonograms through the fetal chest demonstrates a systemic artery (*arrowhead*) arising from the lower thoracic aorta and the pulmonary artery (spectral tracing) supplying the hybrid bronchopulmonary malformation (*asterisks*). Spectral tracing demonstrates both pulmonary arterial supply and pulmonary venous drainage.

Identification of a dilated central bronchus with mucoid impaction suggests CLO. Congenital diaphragmatic hernia (CDH) can usually be differentiated from CPAM by identification of the fetal stomach in the thorax and observation of peristalsis of herniated intestinal loops in the chest. A right-sided CDH associated with liver herniation may appear similar to a microcystic CPAM presenting as a solid intrathoracic mass. In contrast to CPAMs, the herniated liver does not appear as hyperechoic on US. Color Doppler US should correctly diagnose the herniated liver by identifying the intrahepatic portal veins and the inferior vena cava within the mass.

Pulmonary hypoplasia or agenesis may also present with ipsilateral mediastinal shift, thereby mimicking an isoechoic mass such as a CPAM on US.<sup>62</sup> MRI can confirm the correct diagnosis by excluding an underlying lung mass as the cause of the mediastinal shift, thereby confirming the presence of a hypoplastic right lung.

An intrapulmonary bronchogenic cyst is the main differential diagnosis for a macrocystic CPAM. Bronchogenic cysts are usually unilocular cystic lesions, which can occur in the pulmonary parenchyma and are unassociated with a solid component. Lymphatic malformations may also mimic a macrocystic

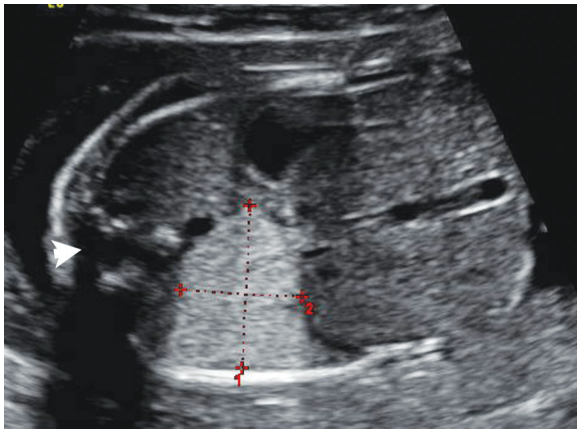


**FIGURE 17.3-11:** Microcystic CPAM at 22 weeks' gestational age. Axial sonogram through the fetal chest demonstrates a hyperechogenic mass (*calipers*) representing a microcystic CPAM. Spine (*arrowhead*).

CPAM, but these lesions almost always originate in an extrathoracic location with secondary invasion into the thorax. The other differential is the rare case of cystic pleuropulmonary blastoma, which is difficult to differentiate from CPAM on imaging.

**Associated Anomalies:** Isolated CPAMs are not associated with increased risk for chromosomal abnormalities<sup>63,64</sup>; however, prenatal series have reported associated anomalies in 8% to 12% of CPAMs. Associated anomalies include renal abnormalities, CDH, tracheoesophageal fistula, and congenital heart defects.<sup>63,65,66</sup> Genetic counseling for fetal karyotyping should be offered when associated anomalies are identified.<sup>67,68</sup>

**Prognosis:** Imaging plays a key role in predicting the clinical outcome for a fetus diagnosed with a CPAM. Prognosis depends on the size of the mass and the presence or absence of hydrops fetalis. Small isolated fetal lung malformations with no mass effect have excellent outcomes and usually are asymptomatic at birth. A subset of fetuses with large CPAMs have mass effect resulting in mediastinal shift and can develop life-threatening complications including hydrops fetalis or, less-commonly, severe pulmonary hypoplasia. Earlier literature reported that 30% to 50% of fetuses with CPAMs developed hydrops fetalis with an associated mortality approaching 100% without intervention.<sup>69</sup> More recent literature suggests that hydrops is less frequent and occurs in 9% to 21% of cases.<sup>70,71</sup> The pathophysiology for hydrops fetalis is felt to be secondary to compression of the heart and inferior vena cava, obstructing venous return

to the heart. Large masses may also be associated with isolated polyhydramnios secondary to compression of the esophagus obstructing normal passage of amniotic fluid into the gastrointestinal tract. In a prospective series, Crombleholme et al.<sup>58</sup> reported that sonographic measurement of the cystic adenomatoid malformation volume ratio (CVR) predicted the risk of hydrops in fetuses with CPAM (aka CCAM). CVR is the measured CPAM volume divided by the head circumference (Fig. 17.3-13). The CPAM volume is a calculated measurement utilizing the formula for a prolate ellipse (mass length  $\times$  height  $\times$  width  $\times$  0.52). In Crombleholme series, a CVR greater than 1.6 predicted an increased risk of hydrops fetalis occurring in 75% of cases.<sup>58</sup> A CVR less than or equal to 1.6 in the absence of a dominant cyst was associated with a less than 3% risk of hydrops fetalis. Crombleholme et al. noted that in addition to the absolute size of the mass, the rate of lesion growth, particularly when associated with a macroscopic cyst, is a risk factor for developing hydrops fetalis.

**Management:** The vast majority of CPAMs are managed conservatively with sonographic surveillance every 1 to 2 weeks to assess for the complication of hydrops fetalis. After 30 weeks' gestational age, the risk of developing hydrops fetalis is unlikely, and the frequency of surveillance can be decreased. Recent literature has suggested that maternal administration of betamethasone for fetuses with large CVRs may have a beneficial effect on microcystic CPAMs in preventing or reversing hydrops fetalis.<sup>72-74</sup> The exact mechanism is unknown, but it is postulated that steroids may accelerate lung maturation or mass involution. Reports from three centers have shown resolution of hydrops fetalis in approximately 80% of CPAMs treated with maternal steroids (Table 17.3-2).<sup>74</sup> In addition, Curran et al.<sup>74</sup> reported survival to discharge ranging from 75% to 100% for large microcystic CPAMs managed with maternal betamethasone. Macrocytic CPAMs do not seem to respond as well to treatment with betamethasone.<sup>72</sup> Loh et al. reported a series comparing steroid treatment to surgical treatment for CPAMs associated with fetal hydrops in the second trimester. Improved survival, particularly for microcystic CPAMs, was noted in the steroid treated group compared with the open surgery group (Table 17.3-3).<sup>75</sup> The current consensus in many centers is to administer maternal steroids as the first line of treatment prior to surgical intervention in fetuses at high risk for fetal hydrops. In fetuses with large CPAMs complicated by hydrops fetalis, who are unresponsive to maternal steroid administration, a spectrum of interventional procedures, including cyst aspiration, placement of a thoracoamniotic shunt, percutaneous laser ablation, or surgical resection, may be considered prior to

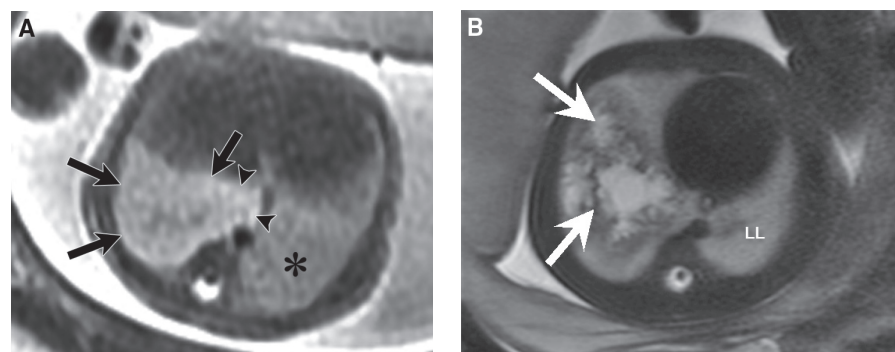


**FIGURE 17.3-12:** MRI appearance of CPAM **A:** Axial T2-weighted MR image of fetus at a gestational age of 22 weeks demonstrates a high-signal intensity CPAM (*arrows*) with small peripheral cysts (*arrowheads*) in the right lower lobe. Normal lung is indicated by *asterisk*. **B:** Axial T2 MRI of fetus at 21 weeks with confirmed CPAM showing complex lesion of mixed signal containing multiple cysts (*arrows*). LL, normal left lung.

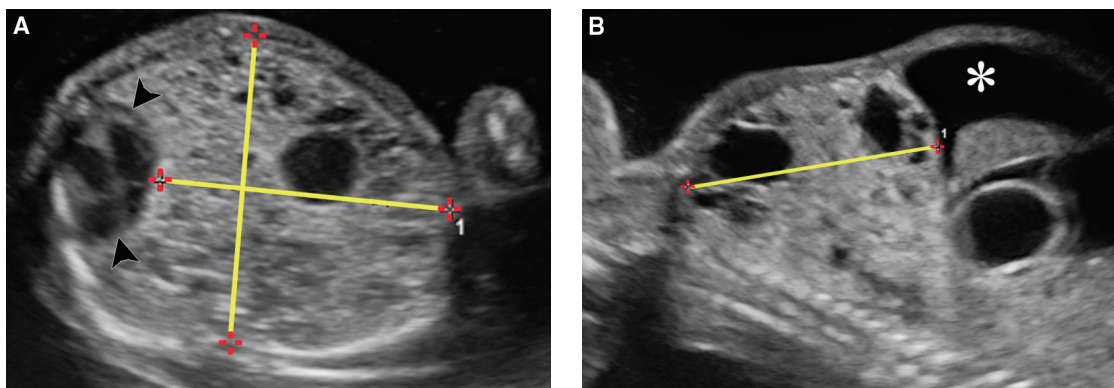


**FIGURE 17.3-13:** CPAM Volume Ratio (CVR): Large CPAM of mixed increased echogenicity and cystic components complicated by early hydrothorax in a 24-week gestational age pregnancy. CPAM volume ratio (CVR) = 2.6. CVR is calculated as the CPAM volume divided by head circumference.  $CVR = L \times H \times W \times 0.52 / \text{head circumference}$ . Axial (**A**) and sagittal (**B**) sonograms demonstrate measurement of the CPAM volume (calipers). Displaced heart is indicated by arrowheads and ascites by asterisk.

**Table 17.3-2** Prenatal Steroids for Microcystic CPAM (Data from Three Centers)

	Patients	CVR	Hydrops	Hydrops Resolved	Survival
UCSF	13	2.7	9 (69%)	7 (78%)	11 (85%)
CHOP	10	2.2	5 (50%)	4 (80%)	10 (100%)
Cincinnati	8	2.5	6 (75%)	5 (83%)	6 (75%)
<b>Total</b>	<b>31</b>	<b>2.5</b>	<b>20/31(65%)</b>	<b>16/20(80%)</b>	<b>27/31(87%)</b>

Adapted from Curran PF, Jelin EB, Rand L, et al. Prenatal steroids for microcystic congenital cystic adenomatoid malformations. *J Pediatr Surg.* 2010;45:145–150.

32 weeks gestational age.<sup>76–79</sup> Open surgery with mass resection has been reported to be approximately 50% successful in managing CPAMs; however, it is controversial because of maternal complications related to the procedure, which include increased risk for premature rupture of the membranes, preterm delivery, and fetal demise.<sup>80</sup> Percutaneous laser ablation of microcystic lesions may be an alternative treatment to surgical resection for microcystic lesions, but additional studies are necessary to consider this as a valid therapeutic option.<sup>81</sup> Fetal percutaneous sclerotherapy has also been reported as a minimally invasive and effective palliative strategy to ameliorate hydrothorax fetalis

associated with predominately solid types of CPAMs, and may represent an alternative to surgical resection.<sup>82</sup>

**Recurrence:** There is no known recurrence risk for isolated CPAM.

### Bronchopulmonary Sequestration

BPSs represent a cystic developmental lung malformation composed of non functioning pulmonary tissue, which lack communication to the tracheobronchial tree and are supplied by a systemic artery.

**Incidence:** BPS is the second most common cause of a congenital lung mass occurring in approximately 1.1% to 1.8% of all pulmonary resections.<sup>83</sup> In the fetus, BPS occurs primarily as an isolated lesion, but can have associated anomalies in approximately 8% of cases and is associated with a CPAM in 25% of cases (see Table 17.3-1).<sup>13</sup>

**Pathogenesis/Associated Anomalies:** BPS is thought to originate from a supernumerary caudally positioned lung bud and has a preferential location for the left lower thorax in 65% to 90% of cases.<sup>83,84</sup> BPSs are characterized as intralobar sequestration (ILS) or extralobar sequestration (ELS).<sup>85</sup> ELS is completely separated from the adjacent normal lung tissue and invested in its own pleural covering. Late development of the lung bud after formation of the pleura leads to formation of a separate pleural

**Table 17.3-3** Steroid Rx vs. Fetal Surgery in 24 Fetuses with CPAM and Fetal Hydrothorax

	Steroid Rx	Surgical Rx
Mean GA age	23 wk	24 wk
CVR	2.68 ± 0.29	2.95 ± 0.31
Survival to delivery	12/13 (92%)	9/11 (82%)
Survival to discharge	10/12 (83%)	5/9 (56%)

Adapted from Loh KC, Jelin E, Hirose S, et al. Microcystic congenital pulmonary airway malformation with hydrothorax fetalis: steroids vs open fetal resection. *J Pediatr Surg.* 2012;47:36–39.

covering surrounding the ELS. ILS shares common pleura with the normal lung tissue. On occasion, ELS and ILS forms of BPS can coexist.<sup>86</sup> ELS accounts for the majority of BPS diagnosed prenatally and approximately 25% to 50% of cases of BPS diagnosed postnatally.<sup>85</sup> Bronchial atresia affecting the lobar, segmental, or subsegmental bronchi has been reported in 100% of ELS and 82% of ILS cases.<sup>53</sup> Approximately 10% to 15% of ELS are found within or below the diaphragm.<sup>84,87</sup> All BPSs receive blood supply from an anomalous systemic feeding artery usually arising from the lower thoracic aorta, upper abdominal aorta, or the celiac artery. Multiple systematic artery feeders may be identified on imaging and at pathology. Venous drainage is via the pulmonary veins in ILS.<sup>88</sup> The venous drainage of ELS is usually systemic through the azygous vein, hemiazygous vein, or the superior vena cava.<sup>83,89</sup> ELS may be associated with other fetal anomalies, most commonly CDH and foregut abnormalities.<sup>84,90</sup>

**Diagnosis:** On US, BPS appears as a homogeneous hyperechoic mass compared with the normal lung in the vast majority of cases (Fig. 17.3-14).<sup>85</sup> Less commonly, there may be a cystic component, with a high percentage attributed to hybrid lesions. Large masses may result in mass effect with mediastinal shift or compression of the diaphragm. BPS are usually detected in the second trimester as an incidental finding and are most commonly localized in the left lower hemithorax or below the diaphragm in approximately 10% of cases.<sup>84,87</sup> Hybrid lesions composed of both CPAM and ELS components are described in approximately 50% of cases (see Fig. 17.3-10).<sup>91,92</sup> A systematic feeding artery or multiple arteries arising from the lower thoracic or abdominal upper aorta can be identified on color

Doppler US in the majority of cases; thereby confirming the diagnosis.<sup>92</sup> On rare occasions, ELS may be complicated by a large ipsilateral hydrothorax, which is thought to occur secondary to torsion of the sequestration, resulting in obstruction of the efferent venous and lymphatic drainage.<sup>93</sup> ELS may be associated with other congenital anomalies, including CDH, cardiac abnormalities, or foregut duplications.<sup>94</sup>

On MRI, BPSs usually appear as a high-signal mass compared with normal fetal lung on T2-fluid sensitive sequences (see Fig. 17.3-14C). The lesions are typically homogeneous high signal intensity and only slightly less intense than that of amniotic fluid. The presence of an associated cyst suggests a hybrid lesion with a CPAM component. Systematic feeding vessels may be identified, usually arising from the lower thoracic or upper abdominal aorta.

**Differential Diagnosis:** Differential diagnosis for an intrathoracic BPS includes other causes of a solid intrathoracic mass—congenital pulmonary airway malformation, congenital lobar or segmental overinflation, and CDH. The identification of a systematic arterial feeder to the BPS should allow for a specific diagnosis. Differential diagnosis for a subdiaphragmatic suprarenal BPS includes adrenal neuroblastoma and adrenal hemorrhage, and again a systemic feeder to a hyperechoic mass in a subdiaphragmatic location should allow for accurate diagnosis of BPS. On MRI, congenital neuroblastoma can appear as a predominantly cystic or solid mass in a fetus. Solid neuroblastomas tend to be heterogeneous with intermediate signal intensity on T2-weighted sequences in contrast to BPS, which are usually high signal intensity lesions on fluid-sensitive T2-weighted MRI sequences. Adrenal hemorrhage is usually diagnosed in

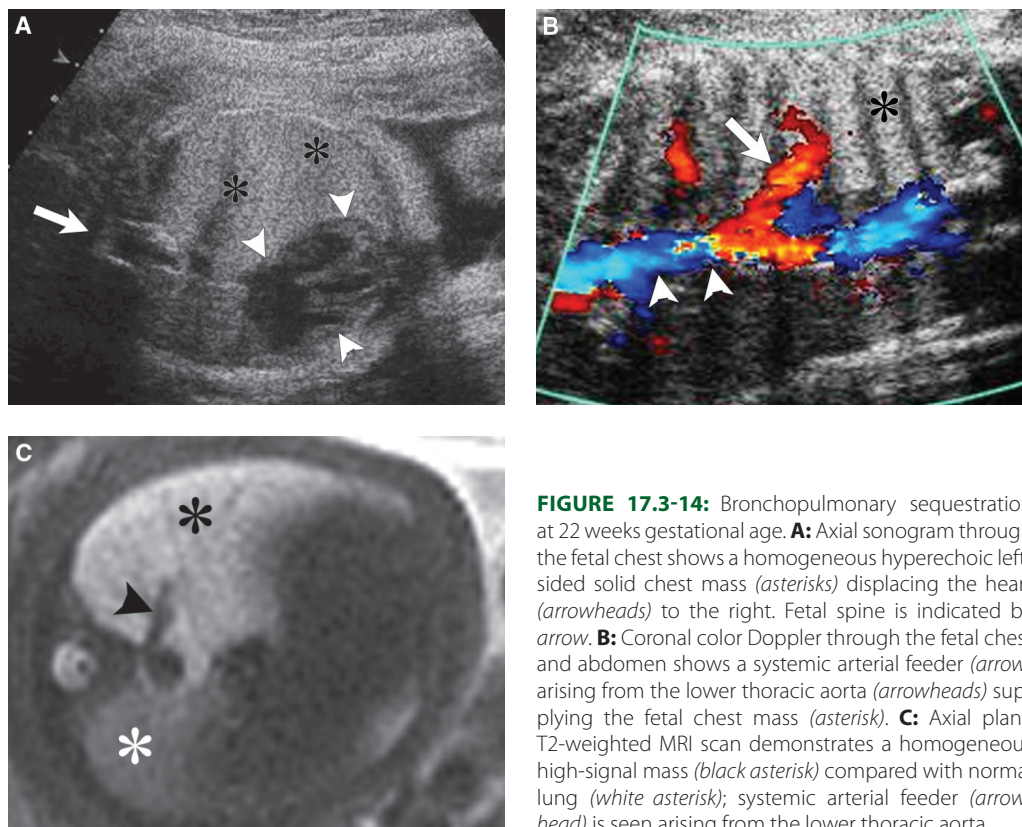


**FIGURE 17.3-14:** Bronchopulmonary sequestration at 22 weeks gestational age. **A:** Axial sonogram through the fetal chest shows a homogeneous hyperechoic left-sided solid chest mass (asterisks) displacing the heart (arrowheads) to the right. Fetal spine is indicated by arrow. **B:** Coronal color Doppler through the fetal chest and abdomen shows a systemic arterial feeder (arrow) arising from the lower thoracic aorta (arrowheads) supplying the fetal chest mass (asterisk). **C:** Axial plane T2-weighted MRI scan demonstrates a homogeneous high-signal mass (black asterisk) compared with normal lung (white asterisk); systemic arterial feeder (arrowhead) is seen arising from the lower thoracic aorta.

the subacute phase and appear as intermediate to high signal on both T2- and T1-weighted sequences.

**Prognosis:** Approximately 68% of BPS lesions regress dramatically before birth, and most are generally associated with an outstanding prognosis.<sup>57</sup> Hydrops fetalis is a rare complication of BPS and much less frequent than in CPAM. ELS may be complicated by a large ipsilateral pleural effusion secondary to torsion, which has a very high mortality in the absence of interventional treatment.

**Management:** Prenatal management consists of surveillance via US. No intervention is required in the vast majority of cases. Early delivery may be contemplated after 32 weeks gestation in the rare case complicated by hydrops fetalis. Thoracoamniotic shunt may be considered for treatment of the infrequent case complicated by a large ipsilateral pleural effusion as the associated mortality is very high in the absence of intervention.<sup>76,78</sup> Open fetal surgical resection is considered controversial because of the maternal risks associated with surgery.

**Recurrence:** There is no known recurrence risk for isolated BPS.

## MASSES

### Pleuropulmonary Blastoma

Pleuropulmonary blastoma (PPB) is also known as pulmonary sarcoma and pulmonary rhabdomyosarcoma.

**Incidence:** PPB is a rare tumor but represents the most common cause of a primary lung malignancy in childhood.<sup>95</sup> The incidence of PPB in the fetus is unknown.

**Pathogenesis:** Although rare, PPB occurs predictably in certain clinical and familial circumstances. Approximately 20% of children with PPB have a family history of pediatric neoplasia, most commonly cystic nephroma of the kidney and rhabdomyosarcoma.<sup>96</sup> PPB families may harbor heterozygous germline mutations in the DICER1 gene, which have been shown to predispose to PPB.<sup>96</sup>

PPB is a dysembryonic malignancy, which is believed to arise from pleuropulmonary germ cells and is composed of both

epithelial and mesenchymal components.<sup>95</sup> Mesenchymal cells susceptible to malignant transformation reside within cyst walls and may evolve into sarcomas. Priest et al.<sup>97</sup> subclassified PPB as type 1 (purely cystic), type 2 (cystic and solid), or type 3 (purely solid) lesions. The type 1 (predominately cystic) lesion represents the early form of the disease and is the type most commonly reported in the fetus or young infant.<sup>97,98</sup> The cystic nature of the mass renders it difficult to distinguish from CPAM as it is pathologically deceptive because of its resemblance to developmental lung cysts.<sup>99</sup> PPB may be unilateral or bilateral.

**Diagnosis:** On imaging with prenatal US or MRI, PPB appears as a primarily cystic or a complex mass with cystic and solid components, which are usually indistinguishable from the findings in congenital pulmonary airway malformation (Fig. 17.3-15). Findings which may help differentiate a PPB from a CPAM include a positive family history, multifocal disease, associated pleural effusion, or continued growth late in gestation past the typical plateau of CPAM growth.<sup>95,100</sup>

**Differential Diagnosis:** Congenital pulmonary airway malformation is the primary differential diagnosis and may appear identical to PPB on prenatal imaging. A positive family history, continued interval growth beyond 28 weeks, and the presence of pleural effusion should raise consideration for a PPB.

**Prognosis:** Complete surgical resection of PPB may be curative, particularly for type 1 (cystic) disease. Type 2 and 3 diseases are often progressive and carry a much worse prognosis.

**Management:** PPB is a very rare lesion in the fetus, and most are presumed to represent a CPAM and, therefore, undergo US surveillance to assess for the complication of hydrops fetalis. In the majority of cases, the diagnosis is not confirmed until after birth, when the lesion is surgically resected. No fetal intervention has been reported in PPB. PPB survival statistics suggest that it is vital to diagnose and treat children at an early age, at which time the lesion is more curable.<sup>99</sup>

**Recurrence:** The recurrence risk for PPB is increased in patients with a familial predisposition associated with the DICER1 gene mutation.<sup>96</sup>

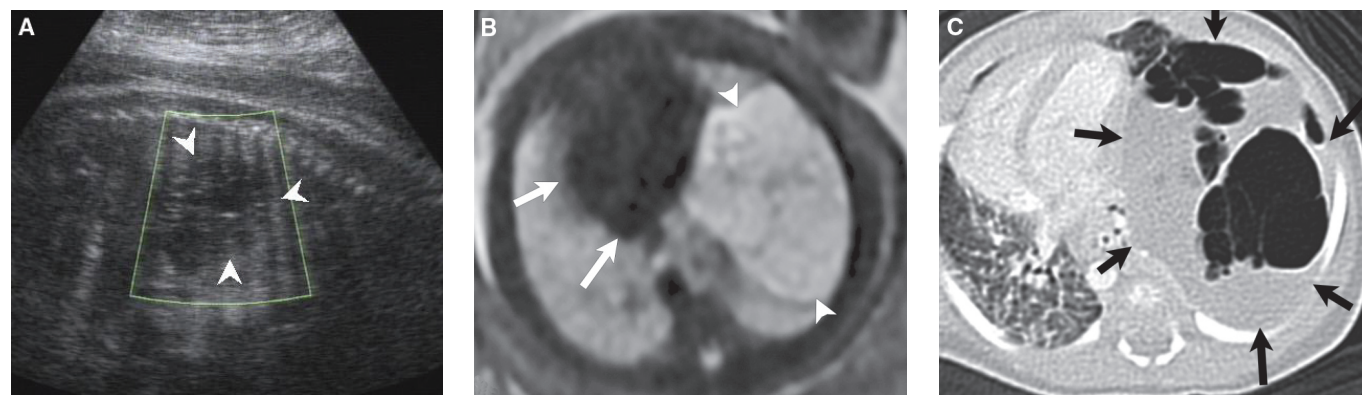


**FIGURE 17.3-15:** Cystic pleuropulmonary blastoma. **A:** Sagittal plane sonogram through the fetal chest demonstrates complex cystic and solid lung mass (*arrowheads*). **B:** Axial T2-weighted MRI demonstrates high-signal mass (*arrowheads*) within the left chest displacing the heart (*arrows*) to the right. **C:** Axial CT scan after birth demonstrates a solid and air-containing cystic mass (*arrows*), confirmed on surgical pathology to represent a cystic pleuropulmonary blastoma. Images courtesy of Beth Kline-Fath, MD.

## MEDIASTINUM

### Thymus

The thymus is a normal lymphoid organ, which is important for immune function during both intrauterine and extrauterine life.<sup>101,102</sup>

**Embryology:** The thymus is derived embryologically from the third pharyngeal pouch and the third pharyngeal cleft, which gives rise respectively to the endodermal (cortical) and ectodermal (medullary) components of the thymus. The pouch is anterior to the aorta in the anterior mediastinum.

**Diagnosis:** On prenatal US, the normal thymus gland can be identified in the majority of fetuses in the second and third trimesters. The thymus gland appears as a bilobed structure in the anterior superior mediastinum ventral to the pericardium and great vessels of the heart. The thymus echogenicity is similar or slightly more echogenic than the fetal lungs early in the second trimester and less echogenic than normal fetal lung tissue in the later part of pregnancy (Fig. 17.3-16A).<sup>103</sup> Occasionally, non-shadowing linear or punctate echogenic foci may be seen in the thymus gland, likely corresponding to normal connective tissue septa and blood vessels. Nomograms for normal fetal thymic size have been reported with no substantial size difference between male and female fetuses.<sup>103-106</sup>

On MRI, the thymus gland should be identified in all normal fetuses in the second and third trimesters with the gland appearing bilobed and intermediate signal intensity on T2-weighted sequences (see Fig. 17.3-16B). The thymus gland is higher in signal than adjacent muscle in the chest wall but of lesser signal intensity than that of adjacent lung tissue in the late second and third trimesters. The two lobes of the thymus gland may substantially differ in size. The normal thymus gland is very pliable, and even when appearing large on US or MRI, does not exhibit compression or displacement of adjacent mediastinal structures.

**Differential Diagnosis:** Solid masses in the thymus gland are extremely rare, and the primary consideration for a solid mass in the anterior/superior mediastinum is a teratoma. Teratomas are usually complex masses with cystic and solid components. Ectopic thyroid or fetal goiter may also mimic a thymic region mass. MRI should accurately characterize the tissue as thyroid gland by identifying the typical bilobed appearance and homogeneous bright signal on T1-weighted sequences. Differential

diagnosis for an apparently absent thymus gland includes ectopic thymus. Early in development, the thymus may fail to normally descend from the neck into the mediastinum as part of normal embryogenesis, in which case the thymus gland can be partially or completely ectopic in the cervical region. The latter is important to recognize as a potential explanation for non visualization of the thymus gland in its expected normal location in the superior mediastinum.<sup>107</sup>

**Associated Anomalies:** Prenatal diagnosis of a thymic mass is a rare occurrence. There have been case reports of prenatally diagnosed thymic cysts. Absence of the thymus gland is indicative of thymic aplasia, and a small gland is associated with thymic hypoplasia (Fig. 17.3-17). These findings are of high concern because of the association in various diseases, including DiGeorge syndrome, Ellis–Van Creveld syndrome, and severe combined immunodeficiency.<sup>108-110</sup> Other associations with an underdeveloped or absent thymus include human immunodeficiency virus, infection, intrauterine growth restriction, acute illnesses, and chorioamnionitis.<sup>111-113</sup> Others have reported that an absent or hypoplastic thymus on US is a marker for deletion 22q11.1 associated with fetal cardiac defects.<sup>114,115</sup> Focused imaging of the thymus gland on US or MRI may be indicated in fetuses at risk for a hypoplastic or absent thymus gland.<sup>104</sup>

### Bronchogenic Cyst

A bronchogenic cyst is a cystic duplication of the tracheobronchial tree.

**Incidence:** Bronchogenic cysts are relatively rare but represent the most common cystic lesion of the mediastinum and account for approximately 20% of surgically resected cystic lung lesions.<sup>116</sup> Prevalence may be underestimated because of cases not coming to clinical recognition.<sup>85</sup>

**Pathogenesis:** Bronchogenic cysts result from abnormal budding of the ventral diverticulum of the foregut, which leads to a focal cystic duplication of the tracheobronchial tree.<sup>85</sup> The cyst walls are lined with ciliated columnar epithelium and often contain fibrous tissue and small amounts of cartilage. Cyst contents may vary from a thin watery fluid collection to thicker mucoid material.<sup>85</sup> The majority of bronchogenic cysts (approximately 85%) are located in the mediastinum most commonly adjacent to the distal trachea or proximal main stem bronchi.

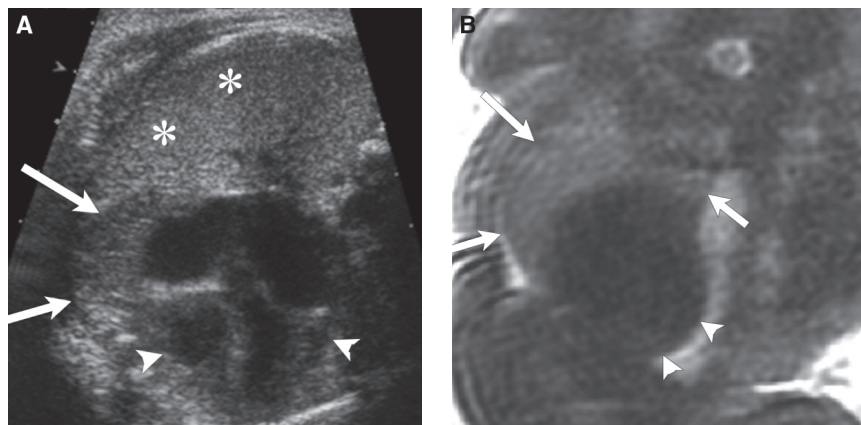


**FIGURE 17.3-16:** Normal thymus gland in third trimester fetus. **A:** Axial sonogram through the chest demonstrates a normal thymus gland (arrows), which is hypoechoic relative to the normal lung (asterisks). Arrowheads indicate the heart. **B:** Coronal T2-weighted MRI through the fetal chest demonstrates the thymus gland as an intermediate signal bilobed structure (arrows). Note normal asymmetry of lobes. Heart is indicated by arrowheads.

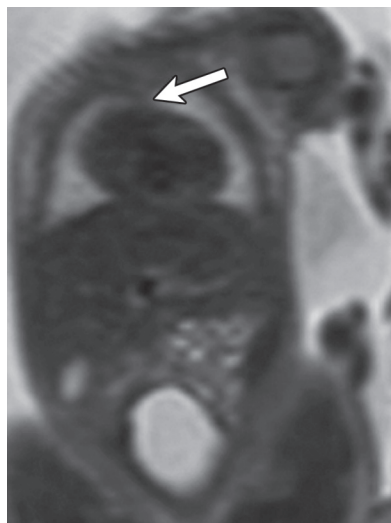


**FIGURE 17.3-17:** Coronal T2-weighted MR image through the fetal chest demonstrates absence of the thymus gland in the superior mediastinum (*arrow*) in a fetus with De George syndrome. (Courtesy of Guillaume Gourincour, MD, Marseille, France.)

The remainder of bronchogenic cysts occur within the lung parenchyma. If the budding abnormality occurs early in bronchial development, the cyst is mediastinal in location, and when abnormal budding occurs later in development, the result is usually an intrapulmonary bronchogenic cyst.<sup>117</sup>

**Diagnosis:** On US, bronchogenic cysts usually appear as a well-defined unilocular hypoechoic mass within the fetal mediastinum near the carina of the trachea or, less commonly, within the lung parenchyma (Fig. 17.3-18A). The cysts are typically solitary or, less commonly, manifest as multiple lesions.<sup>117</sup> Large mediastinal bronchogenic cysts may compress the tracheobronchial tree and esophagus, and result in lung overinflation and polyhydramnios.<sup>118</sup>

On MRI, a bronchogenic cyst appears as a high signal intensity fluid containing structure on T2-weighted sequences (Figs. 17.3-18B and 17.3-19).<sup>119,120</sup> MRI may complement US by ascertaining the precise location of the cyst and assessing for any associated lung parenchyma abnormalities.

**Differential Diagnosis:** The differential diagnosis for a mediastinal bronchogenic cyst includes an enteric duplication cyst involving the esophagus. Enteric duplication cysts are rare congenital anomalies that may arise anywhere in the gastrointestinal tract. Approximately one-third of cases involve the foregut, which includes the esophagus, stomach, and proximal duodenum. A large neurenteric cyst may also mimic a bronchogenic cyst; however, accurate localization of the cyst between the esophagus and the trachea should confirm the correct diagnosis of a bronchogenic cyst. The differential diagnosis for an intrapulmonary bronchogenic cyst includes a unilocular CPAM with a single dominant cyst or the very rare case of a cystic PPB.

**Prognosis:** Limited data are available for the prognosis of prenatally diagnosed bronchogenic cysts. Most lesions are small and unassociated with mass effect, and fare well with no significant complications. Some lesions that compress the bronchial tree may cause overinflation of the adjacent lung parenchyma.

**Management:** Most cysts require no fetal intervention and are managed with serial US to assure stability in size. A very large bronchogenic cyst associated with mediastinal shift may have improved outcome with percutaneous drainage, but the experience is very limited.<sup>118,121</sup>

Most are removed postnatally to prevent superimposed infection, hemorrhage, or growth that could impinge on adjacent structures.

**Recurrence:** There is no known recurrence risk.

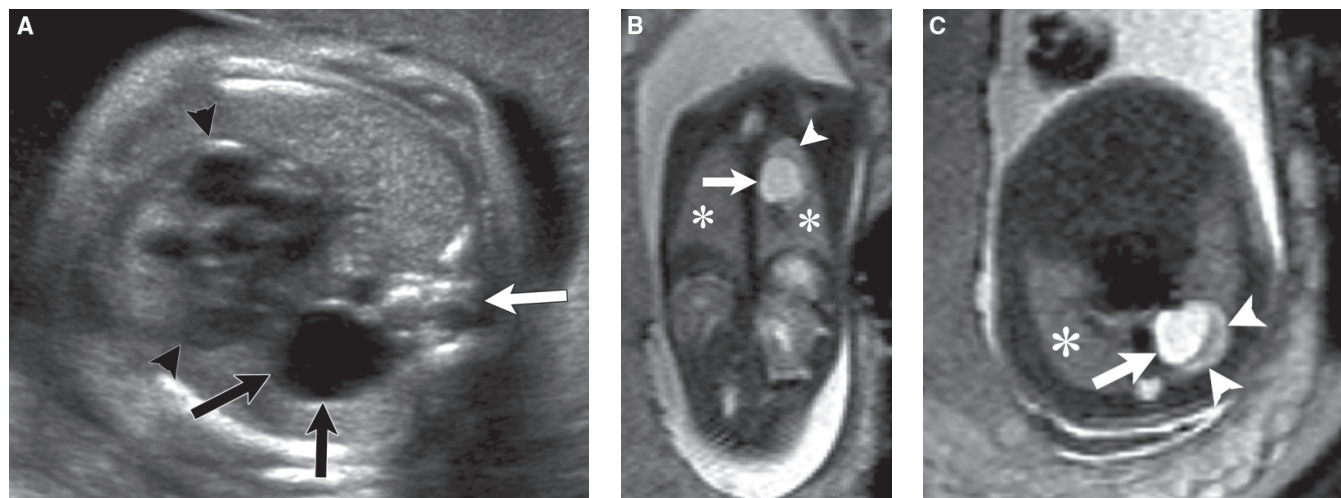


**FIGURE 17.3-18:** Intrapulmonary bronchogenic cyst in 25-week gestational age fetus. **A:** Axial plane sonogram through the fetal chest demonstrates an intrapulmonary unilocular hypoechoic lesion with through transmission (*black arrows*). The heart is indicated by *arrowheads*, and the spine by *white arrow*. Coronal **(B)** and axial **(C)** plane T2-weighted MR images demonstrate a left-sided high-signal mass (*arrow*) confirmed to be a bronchogenic cyst. High signal intensity lung (*arrowheads*) surrounding the cyst corresponded to fluid trapped in the lung distal to the bronchogenic cyst. Normal lungs are indicated by *asterisks*.

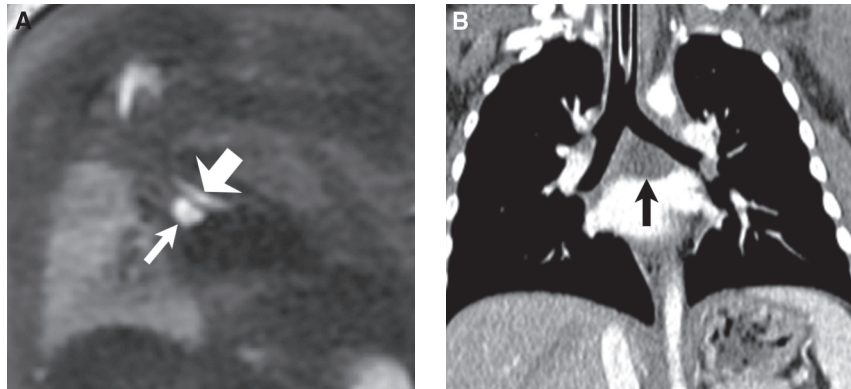


**FIGURE 17.3-19:** Mediastinal bronchogenic cyst causing lung hyperinflation in a 23-week gestational age fetus. **A:** Coronal plane T2-weighted MRI demonstrates a subcarinal bronchogenic cyst (*thin arrow*). Left main stem bronchus is indicated by *thick arrow*. **B:** Newborn coronal plane CT confirms subcarinal bronchogenic cyst (*arrow*).

### Neurenteric Cyst

Neurenteric cysts represent enteric remnants, which result from incomplete separation of the notochord from the foregut during early embryogenesis.<sup>122–124</sup>

**Incidence:** Neurenteric cysts are rare lesions, and the incidence in the fetus is not known.

**Pathogenesis:** Neurenteric cysts are felt to occur due to incomplete notochord separation in the presence of a persistent communication between the ectoderm of the spinal cord and the endoderm of the foregut before closure of the neural tube. Neurenteric cysts are characterized by an intraspinal cystic component that is connected to a mediastinal or thoracic cyst.<sup>125</sup> Approximately 90% of all neurenteric cysts are localized to the posterior mediastinal compartment superior to the carina; however, the cysts may occur at any location throughout the spinal column. The most common locations are in the lower cervical and upper thoracic regions. Most are associated with an intradural extamedullary cystic component within the spinal canal. Connections with the gastrointestinal tract may also be identified.<sup>126</sup> Approximately 50% are associated with vertebral body segmentation anomalies and scoliosis.<sup>122,124,127</sup>

Neurenteric cysts are usually unilocular and appear as a round or tubular mediastinal cystic mass with connection to the spinal canal. Large mediastinal neurenteric cysts may result in mass effect on the adjacent lung, airways, heart, and vessels, and when coexisting with intraspinal lesions may result in signs and symptoms of central nervous system abnormalities after birth.

**Diagnosis:** On US, neurenteric cysts appear as a posterior mediastinal unilocular or septated cyst with a thin wall, most commonly superior to the carina (Fig. 17.3-20A,B). Large cysts with mass effect may result in cardiac malposition or hydrops fetalis. Associated spinal findings include vertebral segmentation anomalies (hemivertebra or butterfly vertebra) and scoliosis.<sup>122,124,127</sup>

On MRI, T2-weighted fluid-sensitive sequences demonstrate a high signal intensity well-margined cyst in the posterior mediastinum (see Fig. 17.3-20B,C). MRI may also show the extent of the lesion into the spinal canal. Neurenteric cysts may be associated with the rare split notochord syndrome characterized by a cleft of the vertebral column. Gastrointestinal and other central nervous system anomalies have been described.<sup>128–130</sup>

**Differential Diagnosis:** Differential diagnosis for a neurenteric cyst includes bronchopulmonary malformations, including a

macrocytic CPAM. Other considerations include a bronchogenic cyst, pericardial cyst, CDH with herniated stomach, and cystic pleural pulmonary blastoma. The presence of associated spinal anomalies should confirm the correct diagnosis of neurenteric cyst.

**Prognosis:** The outcome for a neurenteric cyst depends largely on the extent of the mass, mass effect on adjacent organs, and the presence of associated central nervous system abnormalities. Large cysts may compress the developing lung and result in pulmonary hypoplasia or hydrops fetalis. Pulmonary hypoplasia secondary to a neurenteric cyst can be associated with respiratory distress after birth.<sup>64,127</sup>

**Management:** There is minimal literature regarding the role of surgical intervention in fetuses diagnosed with a neurenteric cyst.<sup>125</sup> Prenatal intervention is rarely indicated, although there have been case reports of treatment by aspiration or placement of a shunt if the cystic mass is large enough to raise concern for pulmonary hypoplasia.<sup>125</sup> Postnatal surgical correction is indicated.

**Recurrence:** The lesion is sporadic with no known recurrence risk.

### Masses-Teratoma

Teratomas are a type of germ cell tumor that histologically contains tissue elements of ectodermal, mesodermal, and endodermal origin.

**Incidence:** Prenatal diagnosis of a mediastinal teratoma is a rare occurrence, and pericardial lesions are extremely rare with fewer than 100 cases reported.<sup>131,132</sup> Teratomas are the most common congenital neoplasm in children, and the vast majority of prenatally diagnosed teratomas are sacrococcygeal, accounting for approximately 80% of all teratomas.<sup>131</sup> Approximately 10% of teratomas are localized in the mediastinum, most commonly in the anterior superior compartment, and when large may result in severe compression of adjacent mediastinal structures and the developing lung.<sup>132</sup>

**Pathogenesis:** Teratomas are neoplasms composed of all three germ layers or multiple foreign tissues without organ specificity. Etiology is yet unknown, but hypothesized to result from aberrant twinning, totipotent cells from Hensen node or from

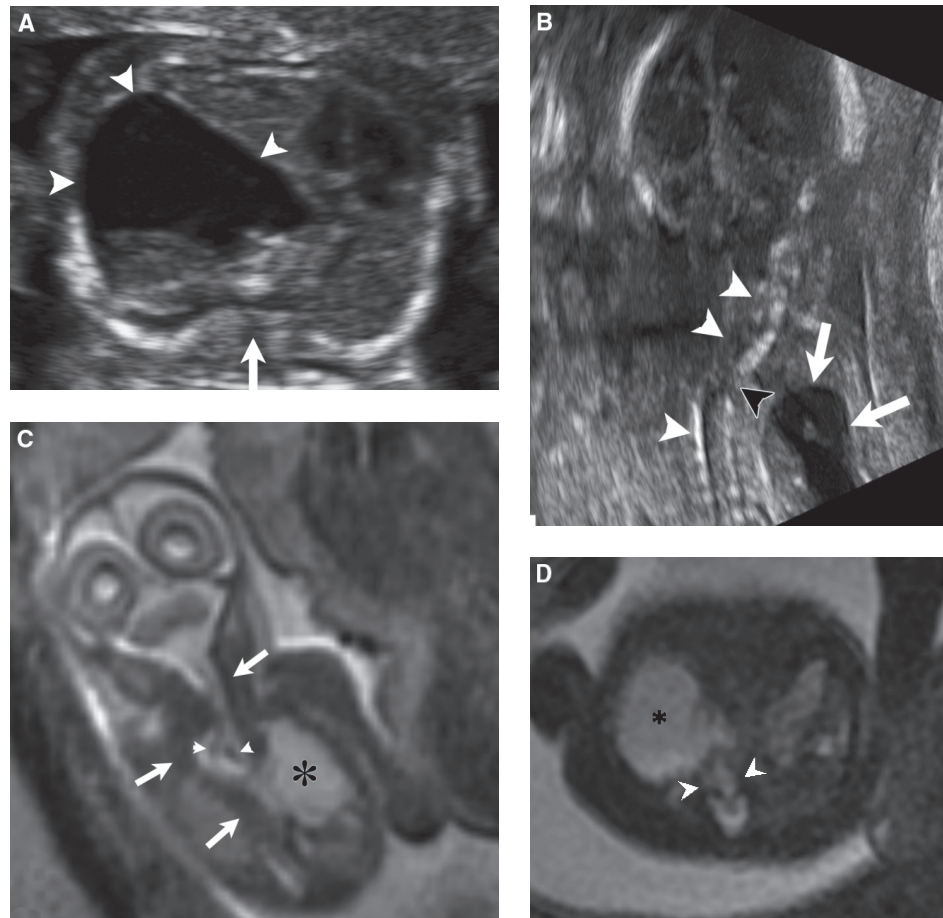


**FIGURE 17.3-20:** Neurenteric cyst. **A:** Axial sonogram shows a large mediastinal cyst (*arrowheads*). Spine is indicated by *arrow*. **B:** Coronal sonogram demonstrates cyst (*arrows*) communicating with spinal canal (*black arrowhead*). Scoliotic spine with abnormal curvature (*white arrowheads*). **C:** Coronal T2-weighted MRI demonstrates split spinal cord (*arrowheads*) and abnormal curvature to the spine (*arrows*). Neurenteric cyst (*asterisk*). **D:** Axial plane SSFP MRI demonstrates neurenteric cyst (*asterisk*) and open communication of spinal canal with posterior mediastinal cyst (*arrowheads*). Images courtesy of Beth Kline-Fath.

reproductive gland analog. The majority of teratomas in children are benign.

**Diagnosis:** On US, mediastinal teratomas are localized to the anterior/superior mediastinum and appear as a cystic, solid, or a complex mass with heterogeneous echogenicity (Fig. 17.3-21A). Hyperechogenic foci associated with acoustic shadowing are indicative of internal calcifications and are helpful to confirm diagnosis. Pericardial teratomas may be differentiated from mediastinal teratoma by the association with pericardial effusion in the majority of cases.<sup>133</sup> On T2-weighted MRI sequences, mediastinal and pericardial teratomas appear as cystic, solid, or complex masses in the superior anterior mediastinum (see Fig. 17.3-21B,C). High-signal foci on T1-weighted sequences are indicative of internal fat, calcification, or hemorrhage into the cystic components. The lesion usually displaces the heart inferiorly.

**Differential Diagnosis:** Differential diagnosis for a mediastinal or pericardial teratoma includes mediastinal bronchogenic cyst or enteric duplication cyst. Bronchogenic cysts or enteric duplication cysts tend to be in the middle or posterior mediastinum respectively and are not associated with solid components.

When large, the lesion may mimic a CPAM, but can be differentiated by inferior more than right or leftward displacement of the heart. The anterior mediastinal location of teratomas and the frequent presence of solid components or calcifications should also allow for accurate diagnosis.

**Prognosis:** Complications of teratomas in the fetus are uncommon, and prognosis is expected to be good for small lesions. Large mediastinal or pericardial teratomas may cause significant mass effect on airway, heart, lungs, and esophagus, resulting in airway obstruction, diminished cardiac output, pulmonary hypoplasia, and polyhydramnios.<sup>132,134</sup> In the presence of polyhydramnios, the fetus is at risk for preterm labor. Hydrops fetalis likely results when a large mass inhibits venous return to the heart and is associated with high morbidity and mortality.<sup>131</sup>

**Management:** Management is surveillance with serial USs to assess for the rare complication of airway obstruction, hydrops fetalis, or diminished cardiac output. If hydrops occurs late in gestation >30 weeks, the fetus may be delivered preterm or EXIT to airway if airway compression is noted.<sup>134</sup> If the fetus is less than 30 weeks with large pericardial effusion or dominant lesion cyst, pericardiocentesis and/or cyst aspiration

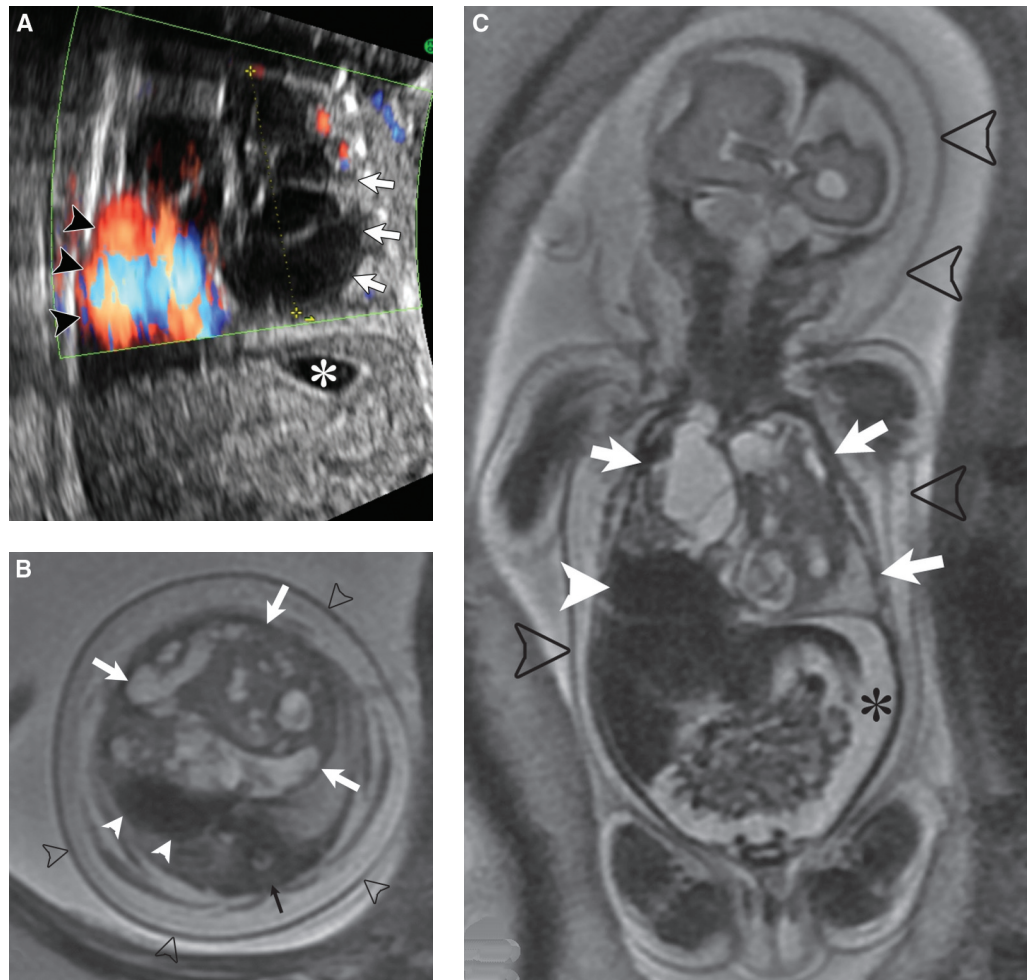


**FIGURE 17.3-21:** Mediastinal teratoma. **A:** Coronal US demonstrates a large complex cystic mediastinal mass (arrows) displacing the heart (arrowheads). Asterisk indicates the stomach. Axial (**B**) and coronal (**C**) T2-weighted MR images demonstrate a large complex mediastinal teratoma (white arrows) displacing the heart (white arrowheads) inferiorly into the right chest and associated fetal hydrops. Skin thickening (black arrowheads) and fetal ascites (black asterisk). Black arrow indicates spine. Images courtesy of Beth Kline-Fath, MD.

may be considered.<sup>135</sup> In the absence of drainable fluid in a severely <30-week hydropic fetus, in utero resection may be attempted. Postnatal resection is mandated because of risk of malignancy.

**Recurrence:** Most cases are sporadic with no recurrence risk; however, there is a small group that is inherited as a familial genetic disturbance.

### Fetal Pleural Effusion (Hydrothorax)

**Incidence:** Fetal pleural effusions are relatively uncommon, manifesting in approximately 1:10,000 to 15,000 pregnancies.<sup>136</sup>

**Pathogenesis:** Fetal pleural effusion may occur as a primary abnormality, usually associated with chylothorax, or as part of hydrops fetalis.<sup>136-140</sup> Most commonly, a pleural effusion in the fetus is associated with hydrops fetalis, which may be caused by numerous conditions, including cardiovascular disease, underlying bronchopulmonary malformations, chromosomal abnormalities (most commonly trisomy 21 and Turner syndrome), CDH, cystic hygroma, or infection.<sup>137-139</sup> Cardiac, pulmonary,

or chromosomal abnormalities are associated in approximately 80% of cases.<sup>137,140</sup>

Maternal parvovirus infection has been associated with transient isolated pleural effusions, which often resolve spontaneously before term and are thought to result from direct pleural inflammation.<sup>141</sup>

Chylothorax is the most common cause of a primary congenital pleural effusion in a fetus and is a diagnosis to be considered after excluding other causes.<sup>142</sup> Chylothorax is commonly due to a primary defect in the lymphatic system, caused either via inflammation or genetic origin or, less likely, as a secondary finding in the presence of an underlying lymphatic malformation. When a primary pleural effusion is large, it may result in mediastinal compression and lead to hydrops fetalis; thereby, making it difficult to distinguish between primary and secondary effusions.<sup>142-144</sup>

**Diagnosis:** On US, fetal pleural effusion is usually detected as an incidental finding by identifying an intrathoracic fluid collection surrounding the fetal lung, most often on the right side but may be bilateral (Fig. 17.3-22). It is often the first sign of fetal hydrops; therefore, identification of pleural effusion should

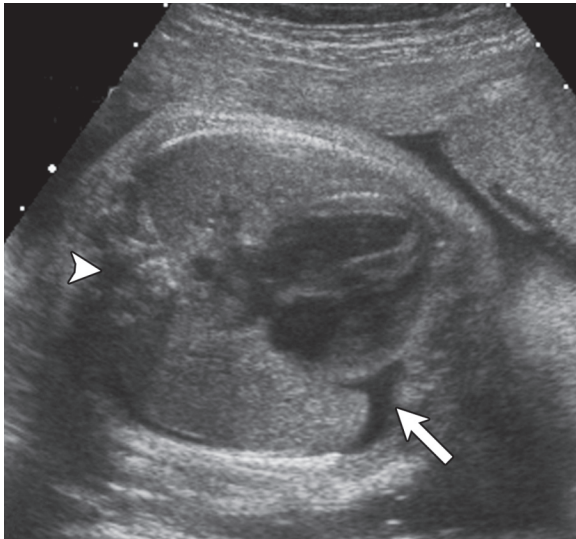


**FIGURE 17.3-22:** Pleural effusion. Axial sonograms demonstrate a right pleural effusion (arrow) secondary to maternal parvovirus infection, which resolved spontaneously without postnatal sequelae. Arrowhead indicates spine.

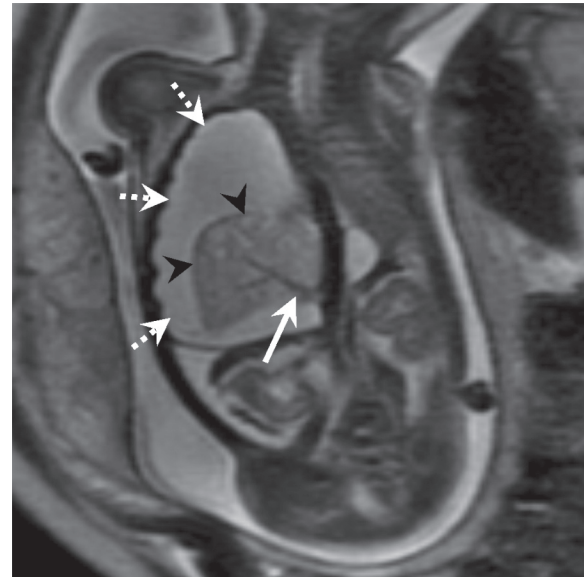


**FIGURE 17.3-23:** A 31-week gestation fetus with large pleural effusion. Coronal T2 MRI identified a heterogeneous lung lesion (arrowheads) supplied by a feeding vessel from aorta (white arrow) in association with large pleural effusion (dotted arrows). Postnatal confirmed hybrid lesion. Images courtesy of Beth Kline-Fath, MD.

trigger an investigation to exclude the more common causes of fetal hydrops prior to assuming the diagnosis of a chylothorax. A search for additional anomalies, including lymphatic malformation or sequestration, should be performed. When pleural effusions are large, the underlying lung will appear to float freely in the pleural cavity.

On MRI, pleural effusions can also be readily identified, which by itself does not add significant information to that provided by US. The potential value of MRI in the setting of a hydrothorax is to identify an associated underlying mass as the etiology of the effusion. For example, torsion of an extralobar sequestration may present with a large ipsilateral pleural effusion (Fig. 17.3-23).

**Differential Diagnosis:** Diagnosis of pleural effusion is usually straightforward. Occasionally, a massive pericardial effusion may mimic a pleural effusion; however, the appearance of the fluid surrounding the heart should allow for distinction. The main challenge in diagnosis of pleural effusion is to distinguish a primary from a secondary effusion. Careful scrutiny to exclude an underlying mass or other anomalies is important for patient counseling and pregnancy management.

**Prognosis:** The prognosis for pleural effusion in the fetus is variable. Some cases resolve or remain stable throughout pregnancy; whereas, others evolve to severe hydrothorax, which can result in hydrops fetalis. Approximately 10% of isolated hydrothoraces resolve spontaneously with good postnatal outcome.<sup>140,142,145</sup> Cases associated with hydrops fetalis have a high mortality rate, reported as greater than 50%.<sup>146</sup> Large bilateral pleural effusions with significant mediastinal compression associated with hydrops fetalis constitute poor prognostic signs with a high likelihood for fatal outcome, reported as greater than 90% in the absence of intervention.<sup>139,143,144,146–151</sup> Large pleural effusions may also compress the underlying lung and result

in pulmonary hypoplasia or compress the esophagus, causing polyhydramnios. Karyotyping to exclude trisomy 21 or Turner syndrome is indicated.

**Management:** Small-to-moderate isolated pleural effusions, which remain stable, can undergo surveillance with serial USs without intervention. Given the high mortality in the presence of large effusions and propensity to develop hydrops, prenatal intervention is typically considered. If the karyotype is normal, maternal diet modification by supplementation with medium-chain triglycerides may decrease or resolve the effusion.<sup>152</sup> If titers are negative for infection and effusion persists, thoracentesis may aid in confirming chylothorax by documenting lymphocyte predominance (>95%).

Thoracoamniotic shunting is the gold standard therapy in the presence of large effusion or hydrops. Shunting may reduce the risk of lung hypoplasia and hydrops and has been reported to improve the outcome.<sup>144,148,149,153,154</sup> With thoracoamniotic shunting, mortality rates are reduced; however, they still remain high at 10% to 30% for non hydropic cases and 50% to 60% for hydropic cases.<sup>142,144,154</sup> Some centers will consider a thoracentesis prior to placing a thoracoamniotic shunt since decompression of fluid may enhance sonographic examination of the fetal heart and the underlying lungs. However, in the majority of cases, the fluid will reaccumulate within 24 hours, and a shunt will need to be placed if prolonged decompression is desired.<sup>142,143,145,155</sup> Recently, pleurodesis with OK-432, a derivative of Group A *Streptococcus pyogenes* treated with penicillin G, has been shown to resolve pleural effusion via inducing sclerosing adhesions. The technique is still investigational and has not yet been proven as effective as thoracoamniotic shunting but may hold promise as an alternative therapy.<sup>152</sup>

**Recurrence:** Risk of recurrence is dependent on the etiology of the effusion. Chylothorax is usually sporadic with low recurrence, although familial cases have been cited.<sup>156</sup>

## REFERENCES

- Lim FY, Crombleholme TM, Hedrick HL, et al. Congenital high airway obstruction syndrome: natural history and management. *J Pediatr Surg*. 2003;38:940–945.
- Barth RA. Imaging of fetal chest masses. *Pediatr Radiol*. 2012;42(suppl 1):S62–S73.
- Gilboa Y, Achiron R, Katorza E, et al. Early sonographic diagnosis of congenital high-airway obstruction syndrome. *Ultrasound Obstet Gynecol*. 2009;33:731–733.
- Vidaeff AC, Szmuk P, Mastrobattista JM, et al. More or less CHAOS: case report and literature review suggesting the existence of a distinct subtype of congenital high airway obstruction syndrome. *Ultrasound Obstet Gynecol*. 2007;30:114–117.
- Kassanos D, Christodoulou CN, Agapitos E, et al. Prenatal ultrasonographic detection of the tracheal atresia sequence. *Ultrasound Obstet Gynecol*. 1997;10:133–136.
- Berg C, Geipel A, Germer U, et al. Prenatal detection of Fraser syndrome without cryptophthalmos: case report and review of the literature. *Ultrasound Obstet Gynecol*. 2001;18:76–80.
- Mong A, Johnson AM, Kramer SS, et al. Congenital high airway obstruction syndrome: MR/US findings, effect on management, and outcome. *Pediatr Radiol*. 2008;38:1171–1179.
- Guimaraes CV, Linam LE, Kline-Fath BM, et al. Prenatal MRI findings of fetuses with congenital high airway obstruction sequence. *Korean J Radiol*. 2009;10:129–134.
- Kohl T, Van de Vondel P, Stressig R, et al. Percutaneous fetoscopic laser decompression of congenital high airway obstruction syndrome (CHAOS) from laryngeal atresia via a single trocar—current technical constraints and potential solutions for future interventions. *Fetal Diagn Ther*. 2009;25:67–71.
- DeCou JM, Jones DC, Jacobs HD, et al. Successful ex utero intrapartum treatment (EXIT) procedure for congenital high airway obstruction syndrome (CHAOS) owing to laryngeal atresia. *J Pediatr Surg*. 1998;33:1563–1565.
- Bui TH, Grunewald C, Frenckner B, et al. Successful EXIT (ex utero intrapartum treatment) procedure in a fetus diagnosed prenatally with congenital high-airway obstruction syndrome due to laryngeal atresia. *Eur J Pediatr Surg*. 2000;10:328–333.
- Langston C. New concepts in the pathology of congenital lung malformations. *Semin Pediatr Surg*. 2003;12:17–37.
- Epelman M, Kreiger PA, Servaes S, et al. Current imaging of prenatally diagnosed congenital lung lesions. *Semin Ultrasound CT MR*. 2010;31:141–157.
- Biyyam DR, Chapman T, Ferguson MR, et al. Congenital lung abnormalities: embryologic features, prenatal diagnosis, and postnatal radiologic-pathologic correlation. *Radiographics*. 2010;30:1721–1738.
- Stigers KB, Woodring JH, Kanga JF. The clinical and imaging spectrum of findings in patients with congenital lobar emphysema. *Pediatr Pulmonol*. 1992;14:160–170.
- Barth RA, Newman B, Rubesova E, et al. Congenital lobar overinflation (CLO)/congenital lobar emphysema (CLE)—not an uncommon cause for a fetal chest mass (Paper # PA9). *Pediatr Radiol*. 2009;39:S255 (Suppl 2):S252.
- Olutoye OO, Coleman BG, Hubbard AM, et al. Prenatal diagnosis and management of congenital lobar emphysema. *J Pediatr Surg*. 2000;35:792–795.
- Pacharn P, Kline-Fath B, Calvo-Garcia M, et al. Congenital lung lesions: comparison between prenatal magnetic resonance imaging (MRI) and postnatal findings. In: Radiological Society of North America 95th Scientific Assembly & Annual Meeting; November 29–December 4, 2009; McCormick Place, Chicago, IL.
- Sparey C, Jawaheer G, Barrett AM, et al. Esophageal atresia in the Northern Region Congenital Anomaly Survey, 1985–1997: prenatal diagnosis and outcome. *Am J Obstet Gynecol*. 2000;182:427–431.
- Depaape A, Dolk H, Lechat MF. The epidemiology of tracheo-oesophageal fistula and oesophageal atresia in Europe: EUROCAT Working Group. *Arch Dis Child*. 1993;68:743–748.
- Torfs CP, Curry CJ, Bateson TF. Population-based study of tracheoesophageal fistula and esophageal atresia. *Teratology*. 1995;52:220–232.
- Forrester MB, Merz RD. Epidemiology of oesophageal atresia and tracheo-oesophageal fistula in Hawaii, 1986–2000. *Public Health*. 2005;119:483–488.
- Pringle KC. Human fetal lung development and related animal models. *Clin Obstet Gynecol*. 1986;29:502–513.
- Slovits TL. *Caffey's Pediatric Diagnostic Imaging*. 11th ed. Philadelphia, PA: Mosby Elsevier; 2008.
- Pameijer CR, Hubbard AM, Coleman B, et al. Combined pure esophageal atresia, duodenal atresia, biliary atresia, and pancreatic ductal atresia: prenatal diagnostic features and review of the literature. *J Pediatr Surg*. 2000;35:745–747.
- Marquette GP, Skoll MA, Yong SL, et al. First-trimester imaging of combined esophageal and duodenal atresia without a tracheoesophageal fistula. *J Ultrasound Med*. 2004;23:1232.
- Estroff JA, Parad RB, Share JC, et al. Second trimester prenatal findings in duodenal and esophageal atresia without tracheoesophageal fistula. *J Ultrasound Med*. 1994;13:375–379.
- Genevieve D, de Pontual L, Amiel J, et al. An overview of isolated and syndromic oesophageal atresia. *Clin Genet*. 2007;71:392–399.
- Holder TM, Cloud DT, Lewis JE Jr, et al. Esophageal atresia and tracheoesophageal fistula: a survey of its members by the Surgical Section of the American Academy of Pediatrics. *Pediatrics*. 1964;34:542–549.
- Bundy AL, Saltzman DH, Emerson D, et al. Sonographic features associated with cleft palate. *J Clin Ultrasound*. 1986;14:486–489.
- Kallen B, Mastroiacovo P, Robert E. Major congenital malformations in Down syndrome. *Am J Med Genet*. 1996;65:160–166.
- Matsuoka S, Takeuchi K, Yamanaka Y, et al. Comparison of magnetic resonance imaging and ultrasonography in the prenatal diagnosis of congenital thoracic abnormalities. *Fetal Diagn Ther*. 2003;18:447–453.
- Satoh S, Takashima T, Takeuchi H, et al. Antenatal sonographic detection of the proximal esophageal segment: specific evidence for congenital esophageal atresia. *J Clin Ultrasound*. 1995;23:419–423.
- Centini G, Rosignoli L, Kenanidis A, et al. Prenatal diagnosis of esophageal atresia with the pouch sign. *Ultrasound Obstet Gynecol*. 2003;21:494–497.
- Stringer MD, McKenna KM, Goldstein RB, et al. Prenatal diagnosis of esophageal atresia. *J Pediatr Surg*. 1995;30:1258–1263.
- Langer JC, Hussain H, Khan A, et al. Prenatal diagnosis of esophageal atresia using sonography and magnetic resonance imaging. *J Pediatr Surg*. 2001;36:804–807.
- Mitani Y, Hasegawa T, Kubota A, et al. Prenatal findings of concomitant duodenal and esophageal atresia without tracheoesophageal fistula (Gross type A). *J Clin Ultrasound*. 2009;37:403–405.
- Levine D, Barnewolt CE, Mehta TS, et al. Fetal thoracic abnormalities: MR imaging. *Radiology*. 2003;228:379–388.
- McKenna KM, Goldstein RB, Stringer MD. Small or absent fetal stomach: prognostic significance. *Radiology*. 1995;197:729–733.
- Brumfield CG, Davis RO, Owen J, et al. Pregnancy outcomes following sonographic nonvisualization of the fetal stomach. *Obstet Gynecol*. 1998;91:905–908.
- Hill LM. Congenital microgastria: absence of the fetal stomach and normal third trimester amniotic fluid volume. *J Ultrasound Med*. 1994;3:894–896.
- Kroes EJ, Festen C. Congenital microgastria: a case report and review of literature. *Pediatr Surg Int*. 1998;13:416–418.
- Menon P, Rao KL, Cutinha HP, et al. Gastric augmentation in isolated congenital microgastria. *J Pediatr Surg*. 2003;38:E4–E6.
- Spitz L. Oesophageal atresia. *Orphanet J Rare Dis*. 2007;2:24.
- Lopez PJ, Keys C, Pierro A, et al. Oesophageal atresia: improved outcome in high-risk groups? *J Pediatr Surg*. 2006;41:331–334.
- Sinha CK, Haider N, Marri RR, et al. Modified prognostic criteria for oesophageal atresia and tracheo-oesophageal fistula. *Eur J Pediatr Surg*. 2007;17:153–157.
- Scott DA. Esophageal atresia/tracheoesophageal fistula overview. In: *GeneReviews* [Internet]. Seattle, WA: University of Washington, Seattle; 2009.
- Burge D, Wheeler R. Increasing incidence of detection of congenital lung lesions. *Pediatr Pulmonol*. 2010;45:103; author reply 104.
- Stocker JT, Madewell JE, Drake RM. Congenital cystic adenomatoid malformation of the lung: classification and morphologic spectrum. *Hum Pathol*. 1977;8:155–171.
- Simonet WS, DeRose ML, Bucay N, et al. Pulmonary malformation in transgenic mice expressing human keratinocyte growth factor in the lung. *Proc Natl Acad Sci U S A*. 1995;92:12461–12465.
- Volpe MV, Pham L, Lessin M, et al. Expression of Hoxb-5 during human lung development and in congenital lung malformations. *Birth Defects Res A Clin Mol Teratol*. 2003;67:550–556.
- Volpe MV, Archavachotikul K, Bhan I, et al. Association of bronchopulmonary sequestration with expression of the homeobox protein Hoxb-5. *J Pediatr Surg*. 2000;35:1817–1819.
- Riedlinger WF, Vargas SO, Jennings RW, et al. Bronchial atresia is common to extralobar sequestration, intralobar sequestration, congenital cystic adenomatoid malformation, and lobar emphysema. *Pediatr Dev Pathol*. 2006;9:361–373.
- Kunisaki SM, Fauza DO, Nemes LP, et al. Bronchial atresia: the hidden pathology within a spectrum of prenatally diagnosed lung masses. *J Pediatr Surg*. 2006;41:61–65.
- Stocker JT. Congenital pulmonary airway malformation: a new name for and an expanded classification of congenital cystic adenomatous malformation of the lung. *Histopathology*. 2002;41:424–431.
- Stocker JT. The respiratory tract. In: Stocker JT, Dehner LP, eds. *Pediatric Pathology*. Philadelphia, PA: Lippincott Williams & Wilkins; 2001:445.
- Adzick NS. Management of fetal lung lesions. *Clin Perinatol*. 2003;30:481–492.
- Crombleholme TM, Coleman B, Hedrick H, et al. Cystic adenomatoid malformation volume ratio predicts outcome in prenatally diagnosed cystic adenomatoid malformation of the lung. *J Pediatr Surg*. 2002;37:331–338.
- Azizkhan RG, Crombleholme TM. Congenital cystic lung disease: contemporary antenatal and postnatal management. *Pediatr Surg Int*. 2008;24:643–657.
- Hubbard AM, Adzick NS, Crombleholme TM, et al. Congenital chest lesions: diagnosis and characterization with prenatal MR imaging. *Radiology*. 1999;212:43–48.
- Hubbard AM. Prenatal magnetic resonance imaging for fetal abnormalities. In: Milunsky A, ed. *Genetic Disorders and the Fetus: Diagnosis, Prevention, and Treatment*. Baltimore and London, UK: Johns Hopkins University Press; 2004:944.
- Abdullah MM, Lacro RV, Smallhorn J, et al. Fetal cardiac dextroposition in the absence of an intrathoracic mass: sign of significant right lung hypoplasia. *J Ultrasound Med*. 2000;19:669–676.

63. Cavoretto P, Molina F, Poggi S, et al. Prenatal diagnosis and outcome of echogenic fetal lung lesions. *Ultrasound Obstet Gynecol.* 2008;32:769–783.
64. Adzick NS, Harrison MR, Crombleholme TM, et al. Fetal lung lesions: management and outcome. *Am J Obstet Gynecol.* 1998;179:884–889.
65. Wilson RD, Hedrick HL, Liechty KW, et al. Cystic adenomatoid malformation of the lung: review of genetics, prenatal diagnosis, and in utero treatment. *Am J Med Genet A.* 2006;140:151–155.
66. Husler MR, Wilson RD, Rychik J, et al. Prenatally diagnosed fetal lung lesions with associated conotruncal heart defects: is there a genetic association? *Prenat Diagn.* 2007;27:1123–1128.
67. Bromley B, Parad R, Estroff JA, et al. Fetal lung masses: prenatal course and outcome. *J Ultrasound Med.* 1995;14:927–936; quiz p1378.
68. Thorpe-Beeston JG, Nicolaides KH. Cystic adenomatoid malformation of the lung: prenatal diagnosis and outcome. *Prenat Diagn.* 1994;14:677–688.
69. Miller JA, Corteveille JE, Langer JC. Congenital cystic adenomatoid malformation in the fetus: natural history and predictors of outcome. *J Pediatr Surg.* 1996;31:805–808.
70. Duncombe GJ, Dickinson JE, Kikiros CS. Prenatal diagnosis and management of congenital cystic adenomatoid malformation of the lung. *Am J Obstet Gynecol.* 2002;187:950–954.
71. Illanes S, Hunter A, Evans M, et al. Prenatal diagnosis of echogenic lung: evolution and outcome. *Ultrasound Obstet Gynecol.* 2005;26:145–149.
72. Morris LM, Lim FY, Livingston JC, et al. High-risk fetal congenital pulmonary airway malformations have a variable response to steroids. *J Pediatr Surg.* 2009;44:60–65.
73. Peranteau WH, Wilson RD, Liechty KW, et al. Effect of maternal betamethasone administration on prenatal congenital cystic adenomatoid malformation growth and fetal survival. *Fetal Diagn Ther.* 2007;22:365–371.
74. Curran PF, Jelin EB, Rand L, et al. Prenatal steroids for microcystic congenital cystic adenomatoid malformations. *J Pediatr Surg.* 2010;45:145–150.
75. Loh KC, Jelin E, Hirose S, et al. Microcystic congenital pulmonary airway malformation with hydrops fetalis: steroids vs open fetal resection. *J Pediatr Surg.* 2012;47:36–39.
76. Brown MF, Lewis D, Brouillette RM, et al. Successful prenatal management of hydrops, caused by congenital cystic adenomatoid malformation, using serial aspirations. *J Pediatr Surg.* 1995;30:1098–1099.
77. Ryo E, Okai T, Namba S, et al. Successful thoracoamniotic shunting using a double-flower catheter in a case of fetal cystic adenomatoid malformation associated with hydrops and polyhydramnios. *Ultrasound Obstet Gynecol.* 1997;10:293–296.
78. Wilson RD, Baxter JK, Johnson MP, et al. Thoracoamniotic shunts: fetal treatment of pleural effusions and congenital cystic adenomatoid malformations. *Fetal Diagn Ther.* 2004;19:413–420.
79. Yokoyama T, Yamashita K, Nishiyama T, et al. A case of thoraco-amniotic shunt for congenital cystic adenomatoid malformation [in Japanese]. *Masui.* 2005;54:287–290.
80. Harrison MR, Adzick NS, Jennings RW, et al. Antenatal intervention for congenital cystic adenomatoid malformation. *Lancet.* 1990;336:965–967.
81. Bruner JP, Jarnagin BK, Reinisch L. Percutaneous laser ablation of fetal congenital cystic adenomatoid malformation: too little, too late? *Fetal Diagn Ther.* 2000;15:359–363.
82. Lee FL, Said N, Grikscheit TC, et al. Treatment of congenital pulmonary airway malformation induced hydrops fetalis via percutaneous sclerotherapy. *Fetal Diagn Ther.* 2012;31:264–268.
83. Rosado-de-Christenson ML, Frazier AA, Stocker JT, et al. From the archives of the AFIP. Extralobar sequestration: radiologic-pathologic correlation. *Radiographics.* 1993;13:425–441.
84. Stocker JT. Sequestrations of the lung. *Semin Diagn Pathol.* 1986;3:106–121.
85. Winters WD, Effmann EL. Congenital masses of the lung: prenatal and postnatal imaging evaluation. *J Thorac Imaging.* 2001;16:196–206.
86. Wesley JR, Heidelberger KP, DiPietro MA, et al. Diagnosis and management of congenital cystic disease of the lung in children. *J Pediatr Surg.* 1986;21:202–207.
87. Lager DJ, Kuper KA, Haake GK. Subdiaphragmatic extralobar pulmonary sequestration. *Arch Pathol Lab Med.* 1991;115:536–538.
88. Johnson AM, Hubbard AM. Congenital anomalies of the fetal/neonatal chest. *Semin Roentgenol.* 2004;39:197–214.
89. Frazier AA, Rosado de Christenson ML, Stocker JT, et al. Intralobar sequestration: radiologic-pathologic correlation. *Radiographics.* 1997;17:725–745.
90. Gerle RD, Jaretzki A III, Ashley CA, et al. Congenital bronchopulmonary-foregut malformation: pulmonary sequestration communicating with the gastrointestinal tract. *N Engl J Med.* 1968;278:1413–1419.
91. Conran RM, Stocker JT. Extralobar sequestration with frequently associated congenital cystic adenomatoid malformation, type 2: report of 50 cases. *Pediatr Dev Pathol.* 1999;2:454–463.
92. Cass DL, Crombleholme TM, Howell LJ, et al. Cystic lung lesions with systemic arterial blood supply: a hybrid of congenital cystic adenomatoid malformation and bronchopulmonary sequestration. *J Pediatr Surg.* 1997;32:986–990.
93. Hernanz-Schulman M, Stein SM, Neblett WW, et al. Pulmonary sequestration: diagnosis with color Doppler sonography and a new theory of associated hydrothorax. *Radiology.* 1991;180:817–821.
94. Newman B. Congenital bronchopulmonary foregut malformations: concepts and controversies. *Pediatr Radiol.* 2006;36:773–791.
95. Priest JR, Williams GM, Hill DA, et al. Pulmonary cysts in early childhood and the risk of malignancy. *Pediatr Pulmonol.* 2009;44:14–30.
96. Hill DA, Ivanovich J, Priest JR, et al. DICER1 mutations in familial pleuropulmonary blastoma. *Science.* 2009;325:965.
97. Priest JR, McDermott MB, Bhatia S, et al. Pleuropulmonary blastoma: a clinicopathologic study of 50 cases. *Cancer.* 1997;80:147–161.
98. Miniati DN, Chintagumpala M, Langston C, et al. Prenatal presentation and outcome of children with pleuropulmonary blastoma. *J Pediatr Surg.* 2006;41:66–71.
99. Hill DA, Jarzembowski JA, Priest JR, et al. Type I pleuropulmonary blastoma: pathology and biology study of 51 cases from the international pleuropulmonary blastoma registry. *Am J Surg Pathol.* 2008;32:282–295.
100. Naffaa LN, Donnelly LF. Imaging findings in pleuropulmonary blastoma. *Pediatr Radiol.* 2005;35:387–391.
101. Haynes BF, Hale LP. The human thymus: a chimeric organ comprised of central and peripheral lymphoid components. *Immunol Res.* 1998;18:175–192.
102. Schwartz RH. Acquisition of immunologic self-tolerance. *Cell.* 1989;57:1073–1081.
103. Cho JY, Min JY, Lee YH, et al. Diameter of the normal fetal thymus on ultrasound. *Ultrasound Obstet Gynecol.* 2007;29:634–638.
104. De Leon-Luis J, Gamez F, Pintado P, et al. Sonographic measurements of the thymus in male and female fetuses. *J Ultrasound Med.* 2009;28:43–48.
105. Felker RE, Cartier MS, Emerson DS, et al. Ultrasound of the fetal thymus. *J Ultrasound Med.* 1989;8:669–673.
106. Li L, Bahtiyar MO, Buhimschi CS, et al. Assessment of the fetal thymus by two- and three-dimensional ultrasound during normal human gestation and in fetuses with congenital heart defects. *Ultrasound Obstet Gynecol.* 2011;37:404–409.
107. Han BK, Yoon HK, Suh YL. Thymic ultrasound, II: diagnosis of aberrant cervical thymus. *Pediatr Radiol.* 2001;31:480–487.
108. Dodson WE, Alexander D, Al-Aish M, et al. The DiGeorge syndrome. *Lancet.* 1969;1:574–575.
109. Ichijima K, Yamabe H, Kobashi Y, et al. An unusual case of metaphyseal chondrodysplasia with an abnormal perilacunar matrix associated with agranulocytosis and hypoplasia of the thymus. *Virchows Arch.* 1981;391:275–289.
110. Martin JP, Aguilar FT. Thymic hypoplasia with severe combined immunodeficiency. *Ann Allergy.* 1977;39:196–200.
111. Hartge R, Jenkins DM, Kohler HG. Low thymic weight in small-for-dates babies. *Eur J Obstet Gynecol Reprod Biol.* 1978;8:153–155.
112. Zalel Y, Gamzu R, Mashiah S, et al. The development of the fetal thymus: an in utero sonographic evaluation. *Prenat Diagn.* 2002;22:114–117.
113. Toti P, De Felice C, Stumpo M, et al. Acute thymic involution in fetuses and neonates with chorioamnionitis. *Hum Pathol.* 2000;31:1121–1128.
114. Chaoui R, Kalache KD, Heling KS, et al. Absent or hypoplastic thymus on ultrasound: a marker for deletion 22q11.2 in fetal cardiac defects. *Ultrasound Obstet Gynecol.* 2002;20:546–552.
115. Barrea C, Yoo SJ, Chitayat D, et al. Assessment of the thymus at echocardiography in fetuses at risk for 22q11.2 deletion. *Prenat Diagn.* 2003;23:9–15.
116. Shanti CM, Klein MD. Cystic lung disease. *Semin Pediatr Surg.* 2008;17:2–8.
117. Young G, L'Heureux PR, Krueckeberg ST, et al. Mediastinal bronchogenic cyst: prenatal sonographic diagnosis. *AJR Am J Roentgenol.* 1989;152:125–127.
118. Barbut J, Fernandez C, Blanc F, et al. Pulmonary sequestration of the left upper lobe associated with a bronchogenic cyst: case report of an exceptional association. *Pediatr Pulmonol.* 2011;46:509–511.
119. Levine D, Jennings R, Barnewolt C, et al. Progressive fetal bronchial obstruction caused by a bronchogenic cyst diagnosed using prenatal MR imaging. *AJR Am J Roentgenol.* 2001;176:49–52.
120. Ward VL. MR imaging in the prenatal diagnosis of fetal chest masses: effects on diagnostic accuracy, clinical decision making, parental understanding, and prediction of neonatal respiratory health outcomes. *Acad Radiol.* 2002;9:1064–1069.
121. Bayar UO, Numanoglu V, Bektas S, et al. Management of fetal bronchogenic lung cysts: a case report and short review of literature. *Case Rep Med.* 2010;2010:751423.
122. Uludag S, Madazli R, Erdogan E, et al. A case of prenatally diagnosed fetal neuroenteric cyst. *Ultrasound Obstet Gynecol.* 2001;18:277–279.
123. Reed JC, Sobonya RE. Morphologic analysis of foregut cysts in the thorax. *AJR Am J Roentgenol.* 1974;120:851–860.
124. Strollo DC, Rosado-de-Christenson ML, Jett JR. Primary mediastinal tumors, part II: tumors of the middle and posterior mediastinum. *Chest.* 1997;112:1344–1357.
125. Aydin AL, Sasani M, Ucar B, et al. Prenatal diagnosis of a large, cervical, intraspinal, neuroenteric cyst and postnatal outcome. *J Pediatr Surg.* 2009;44:1835–1838.
126. Fernandes ET, Custer MD, Burton EM, et al. Neuroenteric cyst: surgery and diagnostic imaging. *J Pediatr Surg.* 1991;26:108–110.
127. Ryckman FC, Rosenkrantz JG. Thoracic surgical problems in infancy and childhood. *Surg Clin North Am.* 1985;65:1423–1454.
128. Perera GB, Milne M. Neuroenteric cyst: antenatal diagnosis by ultrasound. *Australas Radiol.* 1997;41:300–302.
129. Almog B, Leibovitch L, Achiron R. Split notochord syndrome—prenatal ultrasonographic diagnosis. *Prenat Diagn.* 2001;21:1159–1162.
130. Agangi A, Paladini D, Bagolan P, et al. Split notochord syndrome variant: prenatal findings and neonatal management. *Prenat Diagn.* 2005;25:23–27.
131. Schild RL, Plath H, Hofstaetter C, et al. Prenatal diagnosis of a fetal mediastinal teratoma. *Ultrasound Obstet Gynecol.* 1998;12:369–370.

132. Liang RI, Wang P, Chang FM, et al. Prenatal sonographic characteristics and Doppler blood flow study in a case of a large fetal mediastinal teratoma. *Ultrasound Obstet Gynecol.* 1998;11:214–218.
133. Tollens M, Grab D, Lang D, et al. Pericardial teratoma: prenatal diagnosis and course. *Fetal Diagn Ther.* 2003;18:432–436.
134. Merchant A, Hedrick H, Johnson M, et al. Management of fetal mediastinal teratoma. *J Pediatr Surg.* 2005;40:228–231.
135. Takayasu H, Yoshihiro K, Kuroda T, et al. Successful management of a large fetal mediastinal teratoma complicated by hydrops fetalis. *J Pediatr Surg.* 2010;45:621–624.
136. Yinon Y, Grisaru-Granovsky S, Chaddha V, et al. Perinatal outcome following fetal chest shunt insertion for pleural effusion. *Ultrasound Obstet Gynecol.* 2010;36:58–64.
137. Ruano R, Ramalho AS, Cardoso AK, et al. Prenatal diagnosis and natural history of fetuses presenting with pleural effusion. *Prenat Diagn.* 2011;31:496–499.
138. Yinon Y, Kelly E, Ryan G. Fetal pleural effusions. *Best Pract Res Clin Obstet Gynaecol.* 2008;22:77–96.
139. Gratacos E. *Medicina Fetal.* Barcelona: Ed Medica Panamericana (ME); 2007.
140. Aubard Y, Derouineau I, Aubard V, et al. Primary fetal hydrothorax: a literature review and proposed antenatal clinical strategy. *Fetal Diagn Ther.* 1998;13:325–333.
141. Parilla BV, Tamura RK, Ginsberg NA. Association of parvovirus infection with isolated fetal effusions. *Am J Perinatol.* 1997;14:357–358.
142. Deurloo KL, Devlieger R, Lopriore E, et al. Isolated fetal hydrothorax with hydrops: a systematic review of prenatal treatment options. *Prenat Diagn.* 2007;27:893–899.
143. Hayashi S, Sago H, Kitano Y, et al. Fetal pleuroamniotic shunting for bronchopulmonary sequestration with hydrops. *Ultrasound Obstet Gynecol.* 2006;28:963–967.
144. Alkazaleh F, Saleem M, Badran E. Intrathoracic displacement of pleuroamniotic shunt after successful in utero treatment of fetal hydrops secondary to hydrothorax: case report and review of the literature. *Fetal Diagn Ther.* 2009;25:40–43.
145. National Institute for Health and Clinical Excellence. *Insertion of Pleuro-amniotic Shunt for Fetal Pleural Effusion.* London, UK: National Institute for Health and Clinical Excellence; 2006.
146. Longaker MT, Laberge JM, Dansereau J, et al. Primary fetal hydrothorax: natural history and management. *J Pediatr Surg.* 1989;24:573–576.
147. Paladini D, Volpe P. *Ultrasound of Congenital Fetal Anomalies: Differential Diagnosis and Prognostic Indicators.* London, UK: Informa Health Care, Informa UK Ltd; 2007.
148. Blott M, Nicolaides KH, Greenough A. Pleuroamniotic shunting for decompression of fetal pleural effusions. *Obstet Gynecol.* 1988;71:798–800.
149. Rodeck CH, Fisk NM, Fraser DI, et al. Long-term in utero drainage of fetal hydrothorax. *N Engl J Med.* 1988;319:1135–1138.
150. Pumberger W, Hörmann M, Deutinger J, et al. Longitudinal observation of antenatally detected congenital lung malformations (CLM): natural history, clinical outcome and long-term follow-up. *Eur J Cardiothorac Surg.* 2003;24:703–711.
151. Knox EM, Kilby MD, Martin WL, et al. In-utero pulmonary drainage in the management of primary hydrothorax and congenital cystic lung lesion: a systematic review. *Ultrasound Obstet Gynecol.* 2006;28:726–734.
152. Yang Y, Ma G, Shih J, et al. Experimental treatment of bilateral fetal chylothorax using in-utero pleurodesis. *Ultrasound Obstet Gynecol.* 2012;39:56–62.
153. Witlox RS, Lopriore E, Walther FJ, et al. Single-needle laser treatment with drainage of hydrothorax in fetal bronchopulmonary sequestration with hydrops. *Ultrasound Obstet Gynecol.* 2009;34:355–357.
154. Bianchi S, Lista G, Castoldi F, et al. Congenital primary hydrothorax: effect of thoracoamniotic shunting on neonatal clinical outcome. *J Matern Fetal Neonatal Med.* 2010;23:1225–1229.
155. Picone O, Benachi A, Mandelbrot L, et al. Thoracoamniotic shunting for fetal pleural effusions with hydrops. *Am J Obstet Gynecol.* 2004;191:2047–2050.
156. Battin M, Yan J, Aftimos S, et al. Congenital chylothorax in siblings. *Br J Obstet Gynaecol.* 2000;107:1516–1518.